Vibrational properties of a bicrystal interface: Different-interface phonons and the low-temperature specific heat

B. Djafari-Rouhani
Service de Physique Atomique, Section d'Etude, des Interactions Gaz-Solides, Centre d'Etudes Nucléaires de Saclay, Boîte Postale No. 2, 91190 Gif-sur-Yvette, France

P. Masri*
Centre des Mécanismes de la Croissance Cristalline, Université d'Aix-Marseille, Centre de Luminy, 70 route Léon Lachamp, 13288 Marseille Cedex 2, France

L. Dobrzynski
Laboratoire de Physique des Solides,† Institut Supérieur d'Electronique du Nord, 3 rue François Baës, 59046 Lille Cedex, France

(Received 8 June 1976)

The vibrational properties of a coherent interface between two different crystals are studied in this paper on an atomic model. In the long-wavelength approximation, we recover the well-known Stoneley waves of elasticity theory and their existence conditions. We establish also that when these localized Stoneley waves do not exist, one has nevertheless at least one semilocalized acoustic mode (localized in one of the crystals and resonant in the other one). We also report for the first time on a few other interface modes: localized in interface gaps appearing for some values of the propagation vector $k_\parallel$ parallel to the interface; localized, semilocalized, and resonant modes, some of them being in the optically active region. The relations between these different interface modes are discussed. We also derive in this paper for the first time an atomic model's variation in the low-temperature specific heat due to a bicrystal interface and to a planar bulk defect.

I. INTRODUCTION

The vibrational properties of crystal surfaces were extensively studied in the last years, from the theoretical point of view[1] as well as from the experimental one. Analogous studies of a bicrystal interface are still rare. However, the knowledge of the phonons localized at an interface can be useful, for example, in the study of electrical transport through a semiconductor heterojunction, where the electron-phonon coupling plays an important role. This knowledge should give also a better understanding of the crystalline growth. These localized modes can give also a nondispersive phonon propagation at an interface. On the other hand, the recent progress in the fabrication of lamellar crystals and also of small crystalline particles imbedded in another crystal (Guinier-Preston zones, for example) creates systems where the ratio between the number of interface atoms and their total number is non-negligible. It should be possible on such systems to measure the interface specific heat, a quantity we calculate also here for the first time on an atomic model. In this paper, we present also a study of the interface phonons using a well-defined model due to Rosenzweig.[2] In the frame of this model, we obtain the localized and resonant phonons at an interface, as well as their conditions of existence.

Let us describe precisely the model used here. The interface is formed by coupling by their (001) surface two semi-infinite simple cubic crystals A and B. The two crystals are supposed to have the same lattice parameter a. The interactions between the atoms are derived from central potentials between first- and second-nearest neighbors. The force constants between first- and second-nearest neighbors are, respectively, K_i and $\frac{1}{2}K_i$ $(i=A,B)$. The interface coupling is described similarly by K' and $\frac{1}{2}K'$ (see Fig. 1). The crystals A and B are situated, respectively, in the half spaces $l_z \geq 1$ and $l_z \leq 0$, where l_z gives the position of the planes parallel to the interface.

This model was already used[3] to study the interface phonons at a high-symmetry point ($k_x=\pi/a$, $k_y=0$) of the two-dimensional Brillouin zone, and the phonons near a planar defect[4] ($A \equiv B$) along the Δ axis ($0 \leq k_x \leq \pi/a$, $k_y=0$). This last problem was studied before,[5-7] but often using models of the Montroll-Potts type[8] not invariant for the defect atoms under infinitesimal rotation of the whole crystal.[9] The model used here does not have this defect. We study in this paper for the first time the localized and resonant phonons along the Δ axis at a coherent interface between two different crystals. The relations between localized and resonant interface modes are discussed.

In the elastic limit, the model used here was chosen to be isotropic. This combined with the central character of the interactions, yields for each crystal the following relations between the elastic constants:

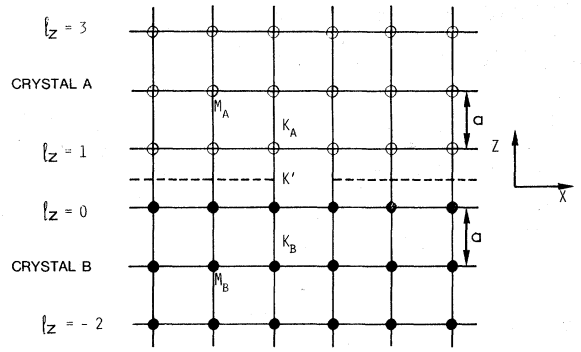

FIG. 1. Schematic representation of the interface model.

$$C_{11} = 3C_{12} = 3C_{44} \quad \text{or} \quad C_l^2 = 3C_t^2,$$

where C_l and C_t are the longitudinal and transverse speeds of sound.

In this limit ($C_l^2 = 3C_t^2$), our results for the localized phonons in the long-wavelength limit agree with the well-known Stoneley[10] waves. In the same limit, the interface specific heat obtained here agrees with the result[11] obtained recently in the frame of the theory of elasticity.

In Sec. II we present the Rosenzweig[2] model and the Green's-function method[12] used to solve our problem. In Secs. III and IV we give the results obtained for the interface waves and the relations between those being localized and those being resonant with bulk waves. In Sec. V, we derive in closed form the low-temperature specific heat of an interface between two different crystals and of a planar defect in a bulk crystal.

II. MODEL

In the Rosenzweig[2] model, along the Δ axis ($k_y = 0$) of the Brillouin zone, the bulk phonon dispersion curves are given by:

$$\omega_{1i}^2(\varphi_z) = \omega_{2i}^2(\varphi_z) = (4K_i/M_i)(2 - \cos\varphi_x - \cos\varphi_z),$$
$$\omega_{3i}^2(\varphi_z) = (4K_i/M_i)(4 - \cos\varphi_x - \cos\varphi_z - 2\cos\varphi_x\cos\varphi_z), \tag{2.1}$$

where M_i is the mass of the atoms in the crystal i ($i = A, B$) and $\vec{\varphi} = \vec{k}a$.

The corresponding eigenvectors are:

$$\vec{e}(\varphi_z, 1) = \left(e_x(\varphi_z, 1) = \left(\frac{(1+\cos\varphi_x)(1-\cos\varphi_z)}{2(1-\cos\varphi_x\cos\varphi_z)}\right)^{1/2},\ e_y(\varphi_z, 1) = 0,\ e_z(\varphi_z, 1) = \left(\frac{(1-\cos\varphi_x)(1+\cos\varphi_z)}{2(1-\cos\varphi_x\cos\varphi_z)}\right)^{1/2}\right),$$
$$\vec{e}(\varphi_z, 2) = (e_x(\varphi_z, 2) = 0,\ \ e_y(\varphi_z, 2) = 1,\ e_z(\varphi_z, 2) = 0),$$
$$\vec{e}(\varphi_z, 3) = (e_x(\varphi_z, 3) = -e_z(\varphi_z, 1),\ \ e_y(\varphi_z, 3) = 0,\ \ e_z(\varphi_z, 3) = e_x(\varphi_x, 1)). \tag{2.2}$$

One sees that along the Δ axis, the phonons of band 2 are polarized along the y axis and are then decoupled from those of bands 1 and 3 polarized in the plane (x, z). This is the main reason why the calculations of the Green's functions can be done in closed form. At points of even higher symmetry like $\varphi_x = 0$ and $\varphi_x = \pi$, the atomic motions along x and z are also decoupled. For $\varphi_x = 0$, band 1 corresponds to the polarization x and band 3 to the polarization z; for $\varphi_x = \pi$, it is the inverse.

For a semi-infinite crystal, one recovers[2] in this model the Rayleigh waves and more generally[13] all along the Δ axis, one has a branch of surface phonons polarized in the sagittal plane (x, z). One has another localized mode polarized in the (x, z) plane and appearing in a gap existing between bands 1 and 3 and also some resonant modes inside the bulk bands. An adsorbed monolayer[13] modifies these modes and can give even new ones.

In the surface studies,[2,13] one finds the frequency of the localized and resonant modes from

$$\mathrm{Re}\Delta_S(\omega^2 + i\epsilon) = 0,$$

with

$$\Delta_S(\omega^2 + i\epsilon) = \det[\vec{\vec{I}} - \vec{\vec{V}}_S \cdot \vec{\vec{G}}_0(\omega^2 + i\epsilon)],$$

$\vec{\vec{G}}_0$ is the bulk Green's function:

$$\vec{\vec{G}}_0(\omega^2 + i\epsilon) = [(\omega^2 + i\epsilon)\vec{\vec{I}} - \vec{\vec{D}}_0]^{-1},$$

where ϵ is an infinitesimal number, $\vec{\vec{I}}$ is the identity matrix, $\vec{\vec{D}}_0$ is the bulk dynamical matrix, and $\vec{\vec{V}}_S$ is the change in $\vec{\vec{D}}_0$ due to the cutting of all the interactions between two adjacent planes. Let $\vec{\vec{D}}$ be the new dynamical matrix, then

$$\vec{\vec{V}}_S = \vec{\vec{D}} - \vec{\vec{D}}_0.$$

Let us now create an interface by coupling two semi-infinite crystals A and B by the interactions K'. The surface modes will be transformed in interface localized and resonant modes. Other modes can also appear, depending on the value of K'. The frequencies of all these modes are solutions of[12]:

$$R(\omega^2) = \mathrm{Re}\Delta(\omega^2 + i\epsilon) = 0\,,$$

with (2.3)

$$\Delta(\omega^2 + i\epsilon) = \det[\vec{\vec{I}} - \vec{\vec{V}}_I \cdot \vec{\vec{G}}(\omega^2 + i\epsilon)]\,,$$

where $\vec{\vec{G}}$ is the Green's function of the two noninteracting semi-infinite crystals and $\vec{\vec{V}}_I$ is the change in their dynamical matrices enabling us to couple them. We calculate Δ analytically in Appendix C.

The variation of the density of states $\Delta n(\omega^2)$ can be calculated[14] from the knowledge of the real part $R(\omega^2)$ and of the imaginary part $J(\omega^2)$ of $\Delta(\omega^2 + i\epsilon)$

$$\Delta n(\omega^2) = \frac{1}{\pi}\frac{d}{d\omega^2}\eta(\omega^2)\,, \tag{2.4}$$

where the phase angle

$$\eta(\omega^2) = -\arg\Delta(\omega^2 + i\epsilon)\,. \tag{2.5}$$

For frequencies near a resonance frequency, $\Delta n(\omega^2)$ can be approximated by the well-known relation[14]

$$\Delta n(\omega^2) \simeq \frac{1}{\pi}\frac{\Gamma}{(\omega^2 - \omega_r^2)^2 + \Gamma^2}, \tag{2.6}$$

where

$$\Gamma = \left.\frac{J}{\partial R/\partial\omega^2}\right|_{\omega^2=\omega_r^2}. \tag{2.7}$$

The resonance is a well-defined feature in the density of states when:

$$\Gamma/\omega_r^2 \ll 1\,. \tag{2.8}$$

Thanks to the decoupling along the Δ axis between the phonons polarized along y and those polarized in the plane (x, z), we have

$$\Delta = \Delta_y \Delta_{xz}\,. \tag{2.9}$$

The coupling $\vec{\vec{V}}_I$ is due to central interactions K' between first- and second-nearest neighbors situated only in the planes $l_z = 0$ and $l_z = 1$. Therefore, for each value of φ_x, we will solve in Sec. III one 2×2 determinant for the y modes and one 4×4 determinant for the xz modes.

III. INTERFACE MODES: ANALYTICAL RESULTS

As seen above [Eq. (2.9)] one can study along the Δ axis, separating the vibrations polarized along y and those polarized in the plane xz. In Sec. III A, we will discuss the y modes and in Secs. III B and III C, the xz modes. In Sec. III B, we make the long-wavelength approximation and recover the Stoneley[10] waves and their existence conditions. Section III C will be devoted to the high-symmetry points ($\varphi_x = \pi$, $\varphi_y = 0$) and ($\varphi_x = \varphi_y = 0$). For the last of these points, we investigate the possibility of an optical interface mode.

In what follows, we use the notations:

$$\alpha_i = K'/K_i \quad (i = A, B)\,, \tag{3.1}$$

$$\delta = (K_A/M_A)(M_B/K_B)\,. \tag{3.2}$$

α_i gives the strength of the interface adhesion. We will consider only $\alpha_i \geq 0$ and will suppose for a given value of $\vec{k}$ that the bulk frequencies in A are lower than those in B $(0 < \delta \leq 1)$.

A. Interface modes polarized along the y axis

For the y-polarized modes, we obtained in Appendix D [Eq. (D5)]:

$$\Delta_y(\varphi_x, \omega) = 1 - \frac{\alpha_A t_A}{t_A - 1} - \frac{\alpha_B t_B}{t_B - 1}, \tag{3.3}$$

where [see Eqs. (D2) and (D3)]:

$$t_i = \begin{cases} \zeta_i - (\zeta_i^2 - 1)^{1/2}, & \text{if } \zeta_i > 1 \\ \zeta_i + i(1 - \zeta_i^2)^{1/2}, & \text{if } -1 < \zeta_i < 1 \\ \zeta_i + (\zeta_i^2 - 1)^{1/2}, & \text{if } \zeta_i < -1 \end{cases} \tag{3.4}$$

and

$$\zeta_i = 2 - \cos\varphi_x - M_i\omega^2/4K_i \quad (i = A, B)\,.$$

We can study now with the help of Eqs. (2.3) and (2.4) the localized and resonant modes having y polarization. They are given by

$$\mathrm{Re}\Delta_y(\varphi_x, \omega) = 0\,.$$

The solutions of this equation will correspond to localized modes if they correspond to frequencies lying outside bands 2 (of polarization y) of the two crystals A and B. This corresponds to $|\zeta_A| > 1$ and $|\zeta_B| > 1$. The solutions correspond to resonant modes (localized at most on one side only of the interface) if the corresponding frequencies are at least inside one of the two bands 2($|\zeta_A| < 1$ or $|\zeta_B| < 1$).

In Fig. 2, we represented these bulk bands 2. Figures 2(a) and 2(b) correspond, respectively, to two different cases for which one has $0.5 < \delta < 1$. Note that when one has $0 < \delta < 0.5$, $\omega_{2B}(0)$ and $\omega_{2A}(\pi)$ cross for a given value of φ_x and a gap (domain 6) appears between the two bulk bands. The localized and resonant modes can be calculated easily from the expression [Eq. (2.3)] in the five regions defined in Figs. 2, as well as in the gap (domain 6).

Region 1. We have $0 < t_i < 1$ and $\Delta > 0$. Then there is no localized mode below the bands.

Region 2. When $\zeta_A = t_A = 1$, let us define

$$\zeta_B^0 = 2 - \cos\varphi_x - \delta(1 - \cos\varphi_x)$$

and

$$t_B^0 = \zeta_B^0 - [(\zeta_B^0)^2 - 1]^{1/2}\,.$$

In the case $0.5<\delta<1$, there exists a resonant mode if

$$\frac{t_B^0}{t_B^0-1}+\frac{K_B}{2K_A}>\frac{K_B}{K'}.$$

For the case $0<\delta<0.5$, we have the same condition when the top limit of this region 2 is $\omega_{2B}(0)$. But when this top limit is $\omega_{2B}(\pi)$, the above condition is replaced by

$$\frac{t_B'}{t_B'-1}+\frac{K_B}{2K_A}<\frac{K_B}{K'}<\frac{t_B^0}{t_B^0-1}+\frac{K_B}{2K_A},$$

where

$$t_B'=\zeta_B'-(\zeta_B'^2-1)^{1/2}$$

and

$$\zeta_B'=2-\cos\varphi_x-\delta(3-\cos\varphi_x).$$

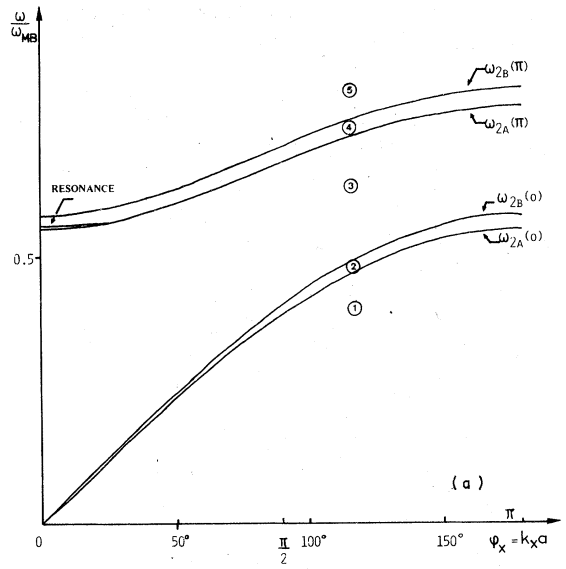

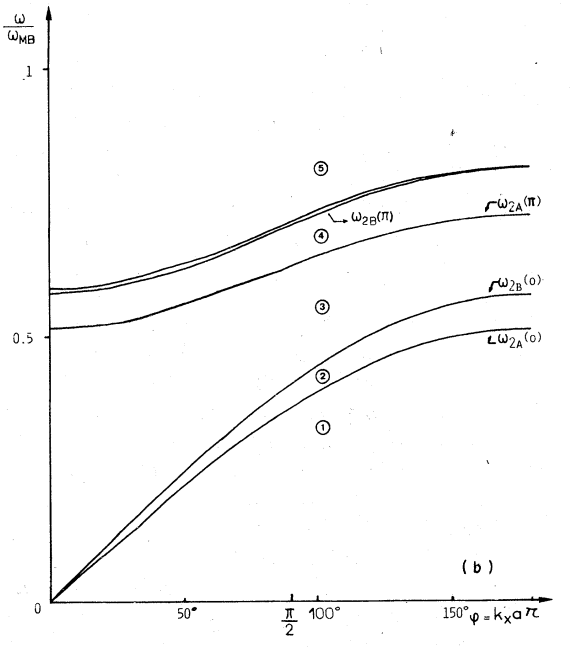

FIG. 2. Transverse interface modes. Limits of the bulk transverse bands are $(\omega_{2A}(0),\ \omega_{2A}(\pi))$ and $(\omega_{2B}(0),\ \omega_{2B}(\pi))$. Figures 2(a) and 2(b) correspond, respectively, to the choice of parameters given by Eqs. (4.1) and (4.2). In Fig. 2(a) one has a semilocalized mode close to $\omega_{2A}(\pi)$ and in Fig. 2(b) a localized mode close to $\omega_{2B}(\pi)$.

Region 3. There is no resonant mode.

Region 4. There exists a resonant mode in the case $0.5<\delta<1$, when

$$\frac{t_A^0}{t_A^0-1}+\frac{K_A}{2K_B}<\frac{K_A}{K'}<\frac{1}{2}+\frac{K_A}{2K_B},$$

where

$$\zeta_A^0=2-\cos\varphi_x-(1/\delta)(3-\cos\varphi_x)$$

and

$$t_A^0=\zeta_A^0+[(\zeta_A^0)^2-1]^{1/2}.$$

An example of such a mode is given in Fig. 2(a). Its dispersion curve is going tangent to $\omega_{2A}(\pi)$ when one is going away from the long-wavelength limit.

In the case $0<\delta<0.5$, we have the same condition when the bottom of region 4 is $\omega_{2A}(\pi)$. But when this bottom is $\omega_{2B}(0)$, the above conditions are replaced by

$$\frac{t_A^0}{t_A^0-1}+\frac{K_A}{2K_B}<\frac{K_A}{K'}<\frac{t_A'}{t_A'-1}+\frac{K_A}{2K_B},$$

where

$$\zeta_A'=2-\cos\varphi_x-(1/\delta)(1-\cos\varphi_x)$$

and

$$t_A'=\zeta_A'+(\zeta_A'^2-1)^{1/2}.$$

Region 5. There exists a localized mode when one has the following condition:

$$\frac{t_A^0}{t_A^0-1}+\frac{K_A}{2K_B}>\frac{K_A}{K'}.$$

An example of such a mode is given in Fig. 2(b).

Region 6. We can have a localized mode in this gap, if

$$\frac{t_B'}{t_B'-1}+\frac{K_B}{2K_A}>\frac{K_B}{K'}.$$

We see now that for a given value of φ_x, one can have zero, one, or two localized or resonant modes; this number depending on the parameters characterizing each crystal, on the interface coupling, and on the value of φ_x. Especially for

$\varphi_x = 0$, one can have only zero or one optical modes. For a given value of φ_x, when the interface coupling is increased, the frequencies of these modes are increasing and new modes may appear.

Let us note also that the phase shift [Eq. (2.5)]:

$$\eta_y(\varphi_x, \omega) = -A\tan \frac{\mathrm{Im}\Delta_y(\varphi_x, \omega)}{\mathrm{Re}\Delta_y(\varphi_x, \omega)} \tag{3.5}$$

has a discontinuous jump of $(\pm\frac{1}{2}\pi)$ when ω crosses $\omega_{iA}(0)$, $i = 1$ or 2, because $\mathrm{Im}\Delta_y$ diverges when $\omega - \omega_{iA}(0) \to +0$.

The results given here for the y modes are interesting by themselves. They can also help to describe other analogous cases. For example, Eqs. (D12), (D13), (D19), and (D20) giving $\Delta_{x \text{ or } z}$ at the high-symmetry points ($\varphi_x = 0$ and π) are formerly identical to the expression of Δ_y [Eq. (3.3)]. Similarly in the Montroll-Potts[8] model, often used to study the qualitative behavior of the vibrational properties, Δ_σ ($\sigma = x, y, z$) can be studied in the whole Brillouin zone in the same manner as here Δ_y is studied [Eq. (3.3)]. The magnetic[15] and electronic[16-18] localized modes at an interface can also be understood by a similar mathematical approach.

B. Sagittal modes and their existence conditions in the elastic limit

In Sec. III A, we saw that there was no y localized mode below the bulk bands. We will study here the sagittal modes polarized in the (x, z) plane in the long-wavelength limit. We will recover the Stoneley wave and its existence condition and show that when the localized Stoneley wave does not exist, a resonant mode appears.

Let us go to the limit $\varphi_x \ll 1$. From Eqs. (2.1), the bulk transverse wave in crystal A can be written

$$\omega_{1A}^2(\varphi_z = 0) = (2K_A/M_A)\varphi_x^2 + O(\varphi_x^4). \tag{3.6}$$

1. Stoneley modes

A localized interface mode will exist if we can find a solution of $\mathrm{Re}\Delta_{xz} = 0$ of the form:

$$\omega^2 = (2K_A/M_A)\gamma\varphi_x^2 + O(\varphi_x^4) \tag{3.7}$$

with $\gamma < 1$.

Let us expand the expression of Δ_{xz} obtained from Eq. (C5) as a function of φ_x. We substitute also to ω^2 its expression (3.7). Finally

$$\Delta_{xz}(\varphi_x, \omega) = \frac{\alpha_B^2 \mathcal{E}(\gamma)}{4\gamma^2 \Delta_A(\gamma)\, \Delta_B(\gamma)} \varphi_x^{-2} + O(\varphi_x^{-1}), \tag{3.8}$$

where

$$\begin{aligned}\mathcal{E}(\gamma) = {} & \left(\frac{K_B}{K_A}\right)^2 F_A G_A \Delta_B(\gamma) \\ & + \frac{K_B}{4\delta K_A}\left[F_A G_B\left(1 - \frac{(G_A - 3I_A)(F_B - 3I_B)}{3\gamma^2\delta}\right)\right. \\ & \left. + F_B G_A\left(1 - \frac{(F_A - 3I_A)(G_B - 3I_B)}{3\gamma^2\delta}\right)\right] \\ & + \frac{F_B G_B \Delta_A(\gamma)}{\delta^2} + O(\varphi_x)\end{aligned} \tag{3.9}$$

and

$$\begin{aligned}F_A &= (1-\gamma)^{1/2} - 3^{1/2}(3-\gamma)^{-1/2}, \\ G_A &= 3^{1/2}(3-\gamma)^{1/2} - 3(1-\gamma)^{-1/2}, \\ I_A &= (1-\gamma)^{1/2} - 3^{-1/2}(3-\gamma)^{1/2},\end{aligned} \tag{3.10}$$

$$\Delta_A(\gamma) = \frac{1}{4}\left(1 + \frac{(F_A - 3I_A)(G_A - 3I_A)}{3\gamma^2}\right) + O(\varphi_x). \tag{3.11}$$

F_B, G_B, I_B, and Δ_B are obtained, respectively, from F_A, G_A, I_A, and Δ_A by replacing γ by $\gamma\delta$. Δ_A and Δ_B are the expressions [Eqs. (B9a) and (B9b)] expanded to order zero.

Let us note that the equations $\Delta_A(\gamma) = 0$ and $\Delta_B(\gamma) = 0$ give, respectively, the Rayleigh waves on the free surface of crystals A and B.

A Stoneley wave will exist when the equation

$$\mathcal{E}(\gamma) = 0 \tag{3.12}$$

has a solution for $\gamma < 1$. The ratio between the speed of this wave and the speed of the bulk transverse wave of crystal A is then $\gamma^{1/2}$.

Let us remark that $\mathcal{E}(\gamma)$ and therefore the frequency of the Stoneley wave are independent of the interface coupling K'. This can be easily understood as the wavelength of these waves is much bigger than the range of this interface coupling. The Stoneley waves depend only on the relative bulk properties of the crystals A and B through the two parameters α_A/α_B and δ (or K_A/K_B and M_A/M_B).

In order to obtain the existence conditions of the Stoneley waves, we put $\gamma = 1$ in Eq. (3.12). In this case, G_A diverges. This is owing to the fact that we kept in the expansions (3.6) and (3.7) of ω_{1A}^2 and ω^2 only the terms of order φ_x^2. If we take into account in the expansions (3.6) and (3.7) the terms of order φ_x^4:

$$\omega_{1A}^2(\varphi_z=0)=\frac{2K_A}{M_A}\varphi_x^2\left(1-\tfrac{1}{12}\varphi_x^2\right)+O(\varphi_x^6), \tag{3.13}$$

$$\omega^2=\frac{2K_A}{M_A}\left(1-A\,\tfrac{1}{12}\varphi_x^2\right)^{\gamma}\varphi_x^2+O(\varphi_x^6), \tag{3.14}$$

then G_A becomes of order φ_x^{-1} by comparison to F_B, G_B, I_B, F_A, I_A. The first-order terms in φ_x in the expansion of $\mathcal{S}$ [Eq. (3.9)] are then those proportional to G_A. Equation (3.12), after division by $G_A[1-(1-\delta)^{1/2}(1-\delta/3)^{1/2}]$ becomes

$$\left(\frac{K_B}{K_A}\right)^2\{(2-\delta)^2-4[(1-\delta)(1-\tfrac{1}{3}\delta)]^{1/2}\}-\frac{K_B}{K_A}\{2(2-\delta)-4[(1-\delta)(1-\tfrac{1}{3}\delta)]^{1/2}+\delta[\tfrac{2}{3}(1-\delta)]^{1/2}\}$$
$$+1-[(1-\delta)(1-\tfrac{1}{3}\delta)]^{1/2}=0. \tag{3.15}$$

The curve defined by Eq. (3.15) bounds the region of existence of the Stoneley waves in the plane $(K_B/K_A, \delta)$, in fact, in the section of this plane corresponding to $0<\delta<1$. An equation analogous to Eq. (3.15) can be deduced for the case $\delta>1$ by replacing in Eq. (3.15) δ by $1/\delta$ and K_B/K_A by K_A/K_B. These results were obtained by Scholte[19] in elasticity theory. The region of existence of these localized waves is displayed in Fig. 3(a) in the plane $(K_B/K_A, M_B/M_A)$: it corresponds to the region inside the curves 1 and 1′. The curve 1 has an asymptote $\delta=0.845$. (Let us remark that this value represents in our model the ratio $C_{RA}^2/C_{tA}^2\equiv C_{RB}^2/C_{tB}^2$, where C_{RA} and C_{RB} are the Rayleigh waves velocity of the crystals A and B, respectively.) The curve 1′ has an horizontal asymptote with $K_B/K_A=2.912$.

We calculated the velocity of the Stoneley waves for $M_A/M_B=2.4$ for values of K_A/K_B satisfying $\delta<1$ [Fig. 3(a)]. The results are given in Fig. 3(b). One sees that, when the bulk bands of crystals A and B are getting closer to one another, then the relative speed of the Stoneley waves $(C_{\text{interface}}/C_{tA})$ decreases.

When the condition [Eq. (3.15)] is exactly satisfied, one can ask if there exists a localized interface mode given by Eq. (3.14) with the constant $A<1$ and $\gamma=1$. However, it seems rather impossible to find two different crystals lying exactly on the boundary of the existence region for Stoneley waves. The only case of practical interest seems to be that of a planar defect in the same crystal $(A\equiv B)$. This case was studied before[4,5] and a localized mode of type [Eq. (3.14) with $\gamma=1$] was found.

2. *Semilocalized interface mode*

In the elastic limit, we investigate also the possibility of existence of a resonant mode of wavelike type in the crystal A, but exponentially damped inside the crystal B. The frequency ω of such a mode has to be inside at least one of the bulk bands of crystal A and outside the bulk bands of crystal B $[\omega_{1A}(0)<\omega<\omega_{1B}(0)]$.

In other words, we look for a solution (3.7) of the equation $\mathrm{Re}\,\Delta_{xz}=0$ but with $1<\gamma<\delta^{-1}$, where δ was defined by Eq. (3.2).

The expression of Δ_{xz} in the long-wavelength limit requires the distinguishing of the two following cases:

(a) $\omega<\omega_{3A}(0)$. This case holds for two possibilities:

$$\omega_{1A}(0)<\omega<\omega_{3A}(0)<\omega_{1B}(0)$$

or

$$\omega_{1A}(0)<\omega<\omega_{1B}(0)<\omega_{3A}(0).$$

Then

$$\Delta_{xz}(\varphi_x,\gamma)=\frac{4-\gamma}{48\gamma^2(\gamma-1)(3-\gamma)}\frac{\alpha_B^2[\mathcal{S}'(\gamma)+i\mathcal{J}'(\gamma)]}{|\Delta_A(\gamma)|^2\Delta_B(\gamma)}\times\varphi_x^{-2}+O(\varphi_x^{-1}), \tag{3.16}$$

where

$$\mathcal{S}'(\gamma)=-3\left(\frac{K_B}{K_A}\right)^2(4-\gamma)\Delta_B(\gamma)+\frac{1}{\delta}\frac{K_B}{K_A}\left(\frac{3^{1/2}(3-\gamma)^{1/2}}{\gamma}[\tfrac{3}{4}(\gamma-2)^2F_B-(\gamma-1)G_B]+\frac{3}{4}\frac{3\gamma^2-10\gamma+4}{\gamma^2\delta}I_B(G_B-F_B)\right)$$
$$+\frac{F_BG_B}{4\gamma^2\delta^2}(3\gamma^3-24\gamma^2+56\gamma-32)+O(\varphi_x), \tag{3.17}$$

$$\mathcal{J}'(\gamma)=3^{1/2}(\gamma-1)^{1/2}(3-\gamma)^{1/2}\times\left\{3\left(\frac{K_B}{K_A}\right)^2(4-\gamma)\Delta_B(\gamma)+\frac{1}{\delta}\frac{K_B}{K_A}\left[-\frac{3^{1/2}(3-\gamma)^{1/2}}{\gamma}\left(+F_B+\frac{(\gamma-2)^2}{4(3-\gamma)}G_B\right)+\frac{3(2-\gamma)}{2\gamma^2\delta}I_B(G_B-F_B)\right]\right\} \tag{3.17′}$$

and

$$\Delta'_A(\gamma) = \frac{\gamma^2 - 4\gamma + 8}{4\gamma^2} - i\,\frac{7\gamma^2 - 28\gamma + 24}{4\sqrt{3}\,\gamma^2(\gamma-1)^{1/2}(3-\gamma)^{1/2}} + O(\varphi_x) \tag{3.18}$$

is the elastic limit expansion of Eq. (B9a) appropriate to the frequency range under study here.

(b) $\omega > \omega_{3A}(0)$. This case holds for:

$$\omega_{1A}(0) < \omega_{3A}(0) < \omega < \omega_{1B}(0)\,.$$

Then

$$\Delta_{xz} = \frac{\alpha_B^2[\mathcal{E}''(\gamma) + i\mathcal{J}''(\gamma)]}{4\gamma^2\Delta''_A(\gamma)\Delta_B(\gamma)}\,\varphi_x^{-2} + O(\varphi_x^{-1})\,, \tag{3.19}$$

where

$$\mathcal{E}''(\gamma) = -3\left(\frac{K_B}{K_A}\right)^2 P_A S_A \Delta_B(\gamma) + \frac{1}{4\gamma^2\delta^2}\,\frac{K_B}{K_A}\,[G_B P_A(F_B - 3I_B)(S_A - T_A) + F_B S_A(G_B - 3I_B)(P_A - 3T_A)]$$
$$+ \delta^{-2}\Delta''_A(\gamma) F_B G_B + O(\varphi_x)\,, \tag{3.20}$$

$$\mathcal{J}''(\gamma) = -\frac{K_B}{K_A}\,\frac{G_B P_A + 3F_B S_A}{4\delta} \tag{3.20'}$$

and

$$P_A = (\gamma-1)^{1/2} + 3^{1/2}(\gamma-3)^{-1/2}\,,$$
$$S_A = (\gamma-1)^{-1/2} + 3^{-1/2}(\gamma-3)^{1/2}\,, \tag{3.21}$$
$$T_A = (\gamma-1)^{1/2} - 3^{-1/2}(\gamma-3)^{1/2}\,,$$
$$\Delta''_A(\gamma) = \tfrac{1}{4}[1 - (1/\gamma^2)(S_A - T_A)(P_A - 3T_A)] + O(\varphi_x)\,. \tag{3.22}$$

As above, $\Delta''_A(\gamma)$ is the elastic limit expansion of Eq. (B9a) appropriate to the frequency range under study here.

Equations analogous to Eqs. (3.16)–(3.22) can be deduced for $\delta > 1$ by replacing in these equations δ by $1/\delta$ and K_B/K_A by K_A/K_B.

With the help of the expressions [Eqs. (3.16)–(3.22)] one can search numerically for a resonant mode for each point of the plane defined by the parameters K_B/K_A and δ. In fact, instead of fixing δ and K_B/K_A and looking for a solution in γ of equation $\mathrm{Re}\,\Delta_{xz} = 0$, it is interesting to note that the expressions (3.17) and (3.20) of $\mathcal{E}'(\gamma)$ and $\mathcal{E}''(\gamma)$ are of second degree with respect of the variable K_B/K_A, then one can choose δ and γ and find the solution of $\mathrm{Re}\,\Delta_{xz} = 0$ in K_B/K_A. Varying δ and γ, we search the region of the plane in Fig. 1(a), where there exist resonant modes. The result of this investigation is the following. When the localized Stoneley wave exists, there is no resonant mode in the elastic limit and for $\omega_{1A}(0) < \omega < \omega_{1B}(0)$.

On the other hand, when there are no Stoneley waves, one has one or three semilocalized interface modes. There are three such modes when the parameters of the two crystals correspond to a point inside the shaded region of Fig. 2(a). (Let us remark that curves 2 and 3 bounding this region when $\delta < 1$ both have the asymptote $\delta = 0.845/3$.) In such a case two of these modes may correspond to an association of a resonance and an antiresonance, which are characterized, respectively, by an increase and a decrease due to the interface in the bulk density of states (see Sec. IV). In fact, in the examples treated in Sec. IV, for which there exists only one resonant mode below $\omega_{1B}(0)$, we shall find (see Figs. 4 and 7) a pair of resonant and antiresonant modes with frequency above $\omega_{1B}(0)$, i.e., outside the region under study here.

Depending upon the relative parameters of the two crystals, these resonances are or are not well-defined features in the density of states. Let us limit ourselves to the half plane $\delta < 1$. Inside the region between curves 1 and 2 [Fig. 2(a)] the quantity $|\Gamma/\omega_r^2|$ [see Eq. (2.8)] corresponding to the single resonant mode can attain values of the order of 0.75, but it can be much smaller, especially in two cases: (i) when the point of interest is near the curve 1, i.e., the solution for the parameter γ defining the velocity of the resonant mode is close to 1; this condition is particularly fulfilled for points for which the parameter δ is itself close to 1. (ii) When K_B/K_A is large; this condition can be realized only if $0.845 \gtrsim \delta \gtrsim 0.845/3$. Between curves 2 and 3 [Fig. 2(a)] there are three resonant modes—the second of these is often well-defined contrary to the two others which are not; nevertheless, when the velocities of two of these modes are close to each other, their widths become very large and diverge even when these two velocities are going to coincide. Finally, in the region above curve 3, the

single resonant mode may be well-defined if the point of interest is far from this curve and/or if $\delta \lesssim 0.845/3$.

Let us illustrate the above considerations by a few examples (the first two are those treated in Sec. IV for all φ_x):

(i) For $M_B/M_A = 1/2.4$, $K_B/K_A = 1/2.2$, there exists a Stoneley wave with $\gamma = 0.993$.

(ii) Putting $M_B/M_A = 1/2.4$, $K_B/K_A = 1/1.9$ we obtain a resonant mode with $\gamma = 1.005$ and $|\Gamma/\omega_r^2| \simeq 0.02$.

(iii) Choosing $M_B/M_A = 1$, $K_B/K_A = 5$ we find first a resonant mode with $\gamma \simeq 2.44$ and $|\Gamma/\omega_r^2| \simeq 0.65$, then an antiresonant mode with $\gamma \simeq 2.97$ and $|\Gamma/\omega_r^2| \simeq 0.06$, and finally a resonant mode with $\gamma \simeq 3.98$ and $|\Gamma/\omega_r^2| \simeq 0.35$.

(iv) For $M_B/M_A = 0.3$, $K_B/K_A = 10$ there exists a resonant mode with $\gamma \simeq 2.42$ and $|\Gamma/\omega_r^2| \simeq 0.53$.

Such semilocalized modes are probably playing an important role when one is generating a Rayleigh wave on a crystal B by transfer[20] from the Rayleigh wave of crystal A.

Let us remark that an interface mode resonant with the bulk phonons of both crystals may exist in the acoustic region corresponding to frequencies $\omega > \omega_{1A}(0)$ and $\omega_{1B}(0)$. The study of such a mode, although cumbersome, may be done in the same way as that of the semilocalized mode. We do not go into this study here as obviously this mode is less interesting from practical point of view (transfer method) than the semilocalized mode. However, in Sec. IV, on two practical examples, we will show the existence of such a well-defined resonance (curves 2 on Figs. 4 and 7).

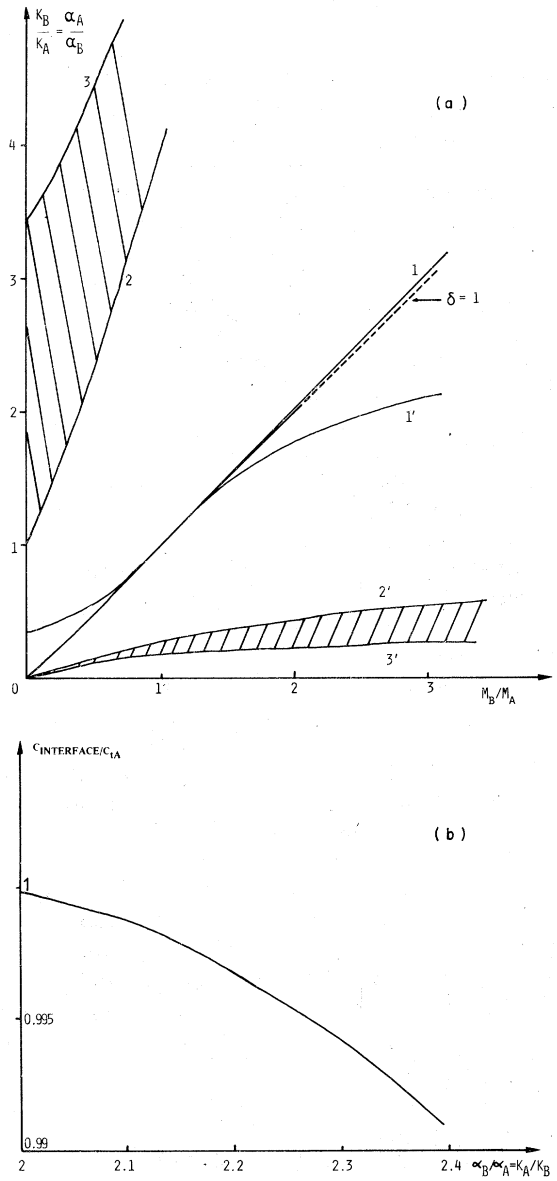

FIG. 3. (a) Stoneley waves exist only in the region between curves 1 and 1′. In the remainder of the plane there exists one resonant (semilocalized) mode in the unshaded region and three such modes in the shaded region. (b) Variation of the ratio between the velocity of the Stoneley wave C_I and the bulk transverse velocity C_{tA} of sound of crystal A, for $M_A/M_B = 2.4$ and in function of K_A/K_B.

C. Interface sagittal modes at limits of the Brillouin zone

It is interesting to study the interface phonons for $\varphi_x = 0$ and $\varphi_x = \pi$ (with still $\varphi_y = 0$), in order to obtain a qualitative feeling about the influence of the interface coupling on these modes. Of course, for $\varphi_x = \pi$ the penetration of the interface modes inside the bulk of the two crystals is of the order of the lattice parameter. Therefore the effect of the interface roughness will be important. We do not go into this problem here.

In Appendix D, we show that for $\varphi_x = 0$ and $\varphi_x = \pi$ (with $\varphi_y = 0$), we have a decoupling between the modes polarized along x and z. For these high-symmetry points $\Delta_{xz} = \Delta_x \Delta_z$. The expressions of Δ_x and Δ_z are derived in Appendix D.

1. Interface modes for $\varphi_x = \pi$ and $\varphi_y = 0$

With the help of Eqs. (D12) and (D13) we can study the existence of these interface modes and their evolution with the strength of the interface coupling K'.

(*a*) *z-polarized modes.* When $K' = 0$, each crystal has a surface mode of polarization z. When K' increases, the frequencies of these modes increase, they enter in resonance with the bulk bands 1 (of polarization z) of the crystals A and B, then they can be localized again above these bulk

bands. When K_B/K_A and δ [Eq. (3.2)] are fixed, we can determine the strength of the coupling K' for which these modes are at the limits of bands 1 of the crystals A and B. Let us illustrate this on the following example for which we choose $K_B/K_A = 1/1.9$ and $\delta^{-1} = 2.4/1.9$. The two surface modes reach $\omega_{1A}(0)$, $\omega_{1B}(0)$, $\omega_{1A}(\pi)$, $\omega_{1B}(\pi)$ for, respectively, $\alpha_B (= K'/K_B) = 0.190$ and 1.453; $\alpha_B = 0.629$ and 2.140; $\alpha_B = 1.071$ and 3.082; $\alpha_B = 1.274$ and 5.103. The full results for this case along the Δ axis will be given for one value of K' in Sec. IV B.

(*b*) *x-polarized modes*. Because of the analogy between $\Delta_x(\pi, \omega)$ [Eq. (D12)] and $\Delta_y(\varphi_x, \omega)$ [Eq. (D5)], one can transpose for this case the results of Sec. III A. There is no localized mode below bulk bands 3 (of polarization x), but one can have for sufficiently high values of the interface coupling K' either resonant modes inside the bulk bands 3 or localized modes above or in between the bulk bands 3. One can have zero, one, or two such modes. When one has two modes, one of them is below $\omega_{3B}(\pi)$ and the other above the highest value of $\omega_{3B}(\pi)$ and $\omega_{3A}(0)$. Finally let us remark that the phase shift $\eta_x(\varphi_x, \omega)$ defined, by analogy with Eq. (3.5), has a discontinuous jump of $+\frac{1}{2}\pi$ or $-\frac{1}{2}\pi$ when ω crosses $\omega_{3A}(\pi)$ or $\omega_{3B}(\pi)$.

2. *Optical interface modes for $\varphi_x = \varphi_y = 0$*

Let us now look for interface modes having a finite frequency for $\varphi_x = \varphi_y = 0$.

The expressions of $\Delta_x(0, \omega)$ and $\Delta_z(0, \omega)$ are given by Eqs. (D19) and (D20) and are again analogous to $\Delta_y(\varphi_x, \omega)$ [Eq. (D5)]. We can therefore transpose to our present study the results of Sec. III A.

(*a*) *z polarized modes*. There is no resonant mode with polarization z below $\omega_{3A}(\pi)$. However, a resonant mode appears between $\omega_{3A}(\pi)$ and $\omega_{3B}(\pi)$ for

$$2\left(1+\frac{K_B}{K_A}\right)^{-1} \leq \frac{K'}{K_A} \leq 2\left(1+\frac{K_B}{K_A}[\delta^{-1}+\delta^{-1/2}(\delta^{-1}-1)^{1/2}]^{-1}\right)^{-1}. \tag{3.23}$$

and a localized mode exists above $\omega_{3B}(\pi)$ if

$$\frac{K'}{K_A} > 2\left(1+\frac{K_B}{K_A}[\delta^{-1}+\delta^{-1/2}(\delta^{-1}-1)^{1/2}]^{-1}\right)^{-1}. \tag{3.24}$$

(*b*) *x polarized modes*. There is no resonant mode below $\omega_{1A}(\pi)$. Such a mode appears between $\omega_{1A}(\pi)$ and $\omega_{1B}(\pi)$ if the condition (3.23) is satisfied. A localized mode exists above $\omega_{1B}(\pi)$ if the inequality [Eq. (3.24)] is fulfilled.

This discussion shows that when the interface coupling is strong enough, optically active interface modes may exist, even when one has two monoatomic crystals. Such interface phonons can couple to photons. Such polaritons have already been observed[21] for lamellar structures formed by two different biatomic crystals.

IV. DISPERSION CURVES OF LOCALIZED AND RESONANT INTERFACE MODES

We obtained in Sec. III the sagittal interface modes in the long-wavelength limit and at a Brillouin zone boundary. In order to obtain the dispersion relations of these modes polarized in the (x, z) plane, we study them here for the first time all along the Δ axis of the Brillouin zone. We saw that there are mainly two distinct possibilities, depending on the existence or nonexistence of the Stoneley wave. We choose therefore: (i) For a case where a Stoneley wave exists

$$K_A/K_B = 2.2, \quad M_A/M_B = 2.4, \quad K'/K_B = 1.4. \tag{4.1}$$

(ii) For a case without a Stoneley wave

$$K_A/K_B = 1.9, \quad M_A/M_B = 2.4, \quad K'/K_B = 1.8. \tag{4.2}$$

The y-polarized modes corresponding to the two above cases were already given in Sec. III A (see Fig. 2).

A. Interface with a Stoneley wave

The dispersion curves of the interface modes are displayed in Fig. 4, where all the frequencies are reported by comparison to ω_{MB}, the maximum bulk frequency of crystal B.

$$\omega_{MB} = (24 K_B/M_B)^{1/2}. \tag{4.3}$$

We obtain a localized mode below the two bulk bands (curve 1), corresponding to the Stoneley wave in the long-wavelength limit.

At higher frequencies, between $\omega_{1B}(0)$ and $\omega_{3A}(0)$, one has a resonance (curve 2), associated to an antiresonance (curve 3). The resonance and the antiresonance are characterized, respectively, by an increase and a decrease due to the interface in the bulk density of states. The surface antiresonances were found before[13] in association with a surface window mode. We call surface window mode a localized mode situated in a gap like AA_1A_2 (see Fig. 4). In Fig. 5(a), we give the generalized partial phase shift[14] [Eq. (2.5)]:

$$\eta_{xz}(\varphi_x, \omega) = -\arg \Delta_{xz}(\varphi_x, \omega)$$

for $\varphi_x = 36°$ and as a function of ω. The resonance

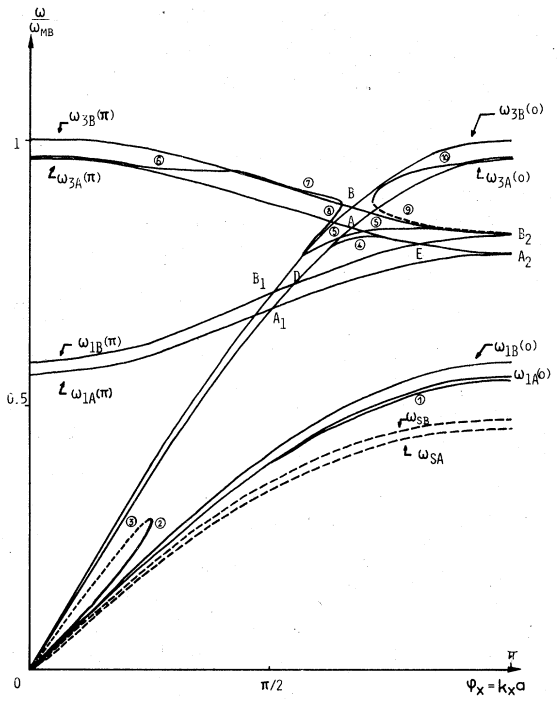

FIG. 4. Different interface modes (1)–(10) polarized in the sagittal plane for the parameters given by Eq. (4.1). Limits of the bulk bands are indicated by $(\omega_{1A}(0), \omega_{1A}(\pi))$, $(\omega_{3A}(0), \omega_{3A}(\pi))$, and similarly for crystal B.

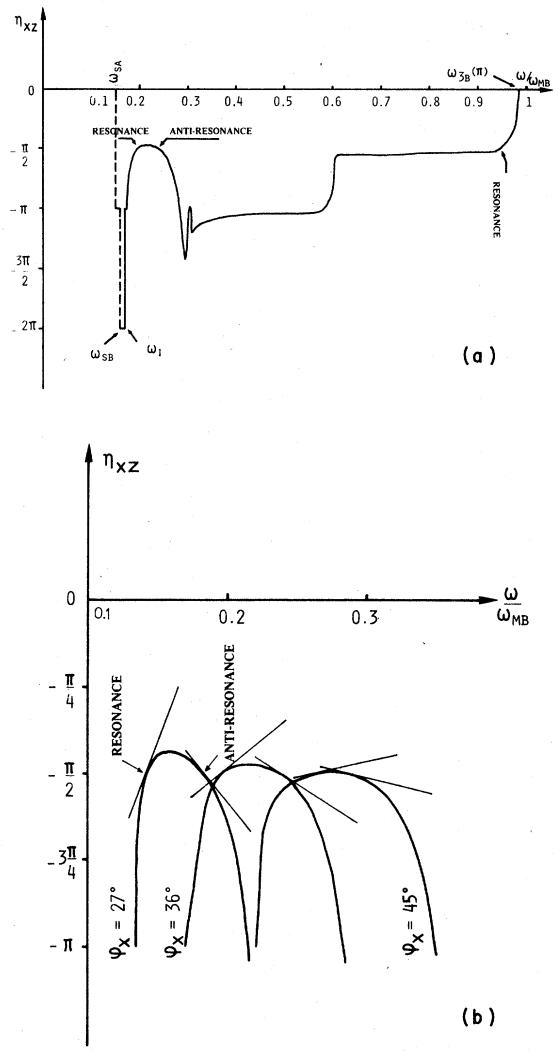

FIG. 5. (a) Partial phase shift $\eta_{xz}(\varphi_x,\omega)$ for $\varphi_x = \frac{1}{5}\pi$ and corresponding to the same choice of parameters Eq. (4.1) as in Fig. 4, ω_{SA} and ω_{SB} are the frequencies of the surface modes of crystal A and B and ω_I is the frequency of the interface mode. (b) Same phase shift as in Fig. 5(a) but near the resonances and for three values of φ_x.

(2) and the antiresonance (3) correspond to a value of this phase shift equal to $-\frac{1}{2}\pi$. In Fig. 5(b), one sees $\eta_{xz}(\varphi_x, \omega)$ near the resonance and the antiresonance for three values of φ_x (27, 36, and 45°). The slope of $\eta_{xz}(\omega)$ at the resonance and at the antiresonance is proportional to the variation of the density of states $\Delta n(\omega)$ [Eq. (2.4)]. One sees from Fig. 5(b) that the resonance (2) and the antiresonance (3) are well-defined features in the density of states unless when φ_x approaches their point of junction $\varphi_J = 45°$.

The intersection ADE of the surface window gaps BB_1B_2 and AA_1A_2 of the two crystals A and B is a gap where interface localized modes may exist. We call this region ADE an interface window gap. In AA_1A_2 and BB_1B_2 there exist surface window modes.[13] Once the two crystals A and B are coupled, we are getting interface window modes in the window ADE. In the present case we have two such modes [curves (4) and (5)]. The mode (5) is localized in the window ADE and semilocalized (resonant with bulk modes of crystal A) in the surface window BB_1B_2. This semilocalized mode intersects $\omega_{3A}(\pi)$ for $\varphi_x = 125°$. Using Eqs. (2.6)–(2.8) we studied the definition in frequency of this mode. The results are given in Fig. 6(a). One sees that $|\Gamma/\omega_r^2|$ is of the order of 0.01 and is going to zero like $J(\omega_r)$ when one approaches the point S where this mode falls into the interface window ADE. This semilocalized mode is therefore a well-defined feature especially near the S point.

We obtain also a semilocalized mode of optical character [curve (6)] between $\omega_{3A}(\pi)$ and $\omega_{3B}(\pi)$. This mode intersects $\omega_{3B}(\pi)$ for $\varphi_x \simeq 0.47\pi$ and then becomes localized [curve (7)]. We give in Fig. 6(b) the variations of $|\Gamma/\omega_r^2|$, $J(\omega_r)$, and $(\partial R/\partial \omega^2)_{\omega^2 = \omega_r^2}$ as a function of φ_x when mode (6) ap

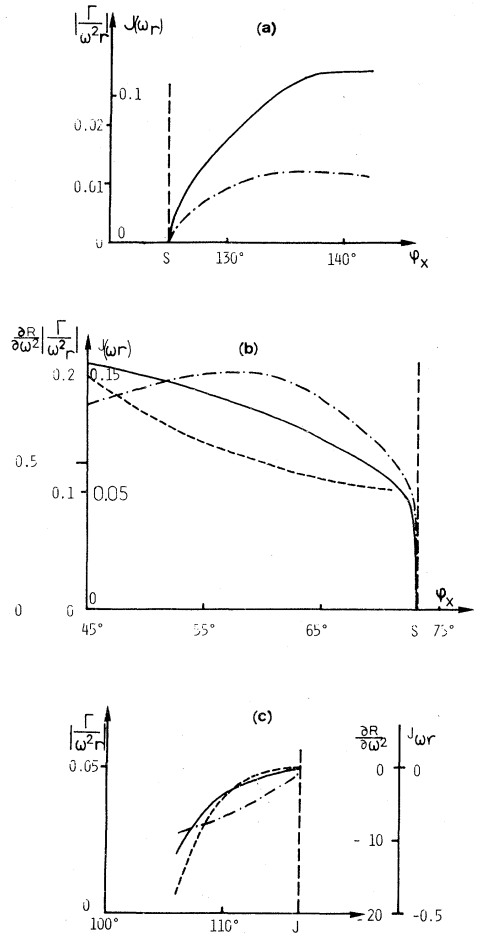

FIG. 6. Study of the definition of some of the semilocalized and resonant modes given in Fig. 4. $J(\omega)$ and $R(\omega)$ are, respectively, the imaginary and real parts of $\Delta(\omega)$ given by Eq. (2.3). Modes are well defined when $|\Gamma/\omega_r^2| \ll 1$, where $\Gamma = J/(\partial R/\partial\omega^2)|\omega^2=\omega_r^2$. (a) Mode (5); (b) mode (6); (c) mode (8). Full, dash-dotted and dashed lines give, respectively, $J(\omega_r)$, $|\Gamma/\omega_r^2|$, and $\partial R/\partial\omega^2$.

proaches the point S where it merges into mode (7). Mode (6) appears to be relatively well defined ($\Gamma/\omega_r^2 \simeq 0.2$) and very well defined near S where $\partial R/\partial\omega^2$ is slowly varying and $|\Gamma/\omega_r^2|$ is going to zero like $J(\omega_r)$.

For $0.57\pi < \varphi_x < 0.65\pi$, mode (7) is associated with a partially semilocalized and resonant mode [curve (8)]. The definition of this mode (8) is studied in Fig. 6(c). It is formed to be well defined. Near the point J where it merges into mode (7), $J(\omega_r)$ and $\partial R/\partial\omega^2$ vary linearly with φ_x, and Γ/ω_r^2 is going to a finite value of the order of 0.05. The sharpness of the peak in the density of states is then more important near J for mode (8) than near S for mode (6).

One has also near $\varphi_x = \pi$ a semilocalized mode (10) associated with an antiresonance (9). The mode (10) is very close to $\omega_{3A}(0)$ for φ_x going to π.

B. Interface without a Stoneley wave

Let us first note that with the choice of parameters given by Eq. (4.2), the frequency $\omega_{SB}(\varphi_x)$ of the surface mode of the crystal B is in the long-wavelength limit between $\omega_{1A}(0)$ and $\omega_{1B}(0)$; more precisely

$$\frac{\omega_{SB}^2}{\omega_{MB}^2} \simeq \frac{0.845\varphi_x^2}{12} \quad \text{and} \quad \frac{\omega_{1A}^2(0)}{\omega_{MB}^2} \simeq \frac{0.792\varphi_x^2}{12} .$$

But outside the long-wavelength limit, $\omega_{SB}(\varphi_x)$ is below $\omega_{1A}(0)$.

The semilocalized acoustic mode found in Sec. III B 2 (see Fig. 7) is here very close to ω_{SB}. Then it crosses $\omega_{1A}(0)$ and becomes localized. Its frequency is beginning to be sensibly different from ω_{SB} for $\varphi_x = 0.67\pi$. Finally this localized mode is getting semilocalized again for $0.7\pi < \varphi_x < \pi$ [curve (1)]. The definition of this mode (1) is studied in Fig. 8(a): Γ/ω_r^2 is of the order of 0.2 and this mode is rather well defined. Near point S where this mode becomes localized, $J(\omega_r)$ is going to

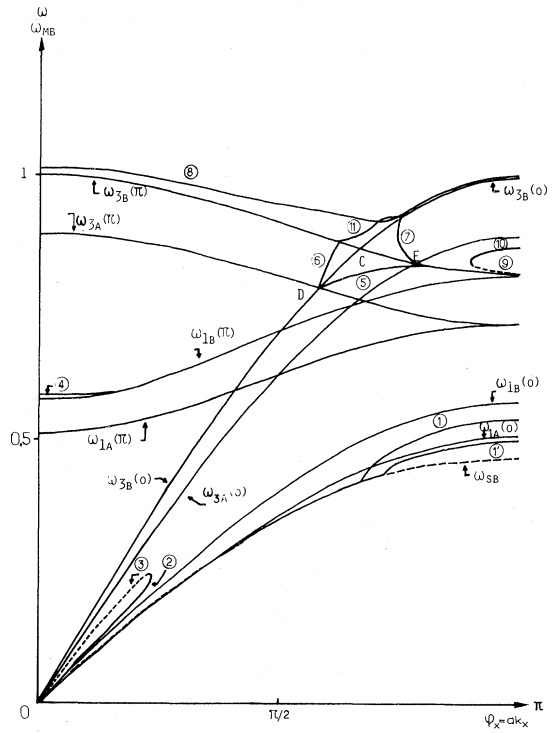

FIG. 7. Different interface modes [(1)–(11)] polarized in the sagittal plane for the parameters given by Eq. (4.2). Limits of the bulk bands are indicated by ($\omega_{1A}(0)$, $\omega_{1A}(\pi)$), ($\omega_{3A}(0)$, $\omega_{3A}(\pi)$), and similarly for the crystal B.

zero and $\partial R/\partial \omega^2$ to a nonzero value. The semilocalized mode is going to a $\delta(\omega)$ peak at the point S. When the interface coupling is decreased ($\alpha_B = 1.1$), this mode (1) becomes localized [curve (1′)] and is again very close to $\omega_{SB}(\varphi_x)$ for $\varphi_x \lesssim 130°$.

Between $\omega_{1B}(0)$ and $\omega_{3A}(0)$ (see Fig. 7), we have a resonance [curve (2)] and an antiresonance [curve (3)] similar to the ones discussed in Sec. IV A (Fig. 4). From Fig. 8(b), we are getting the same conclusions about the definition of these modes as those we reached from Fig. 5(b) in Sec. IV A, especially near the point J where the resonance and the antiresonance are meeting.

Inside the bulk bands 3 of the two crystals, we have a resonance [curve (4)] of optical type. Its frequency is above $\omega_{1B}(\pi)$. To this resonance is associated an antiresonance lying very close to $\omega_{1B}(\pi)$. We represented it in Fig. 9(a). The definition of these modes can be understood from Fig. 9(b) where we give the partial phase shift $\eta_{xx}(\varphi_x, \omega)$ for three values of φ_x. These two modes have the same qualitative behavior as modes (2) and (3).

Inside the interface window CDE (Fig. 7), we have a localized mode [curve (5)]. This mode exists for $105 < \varphi_x < 112°$ together with the semilocalized mode (6). For $\varphi_x = 112°$, mode (6) is getting localized [curve (11)]. Mode (11) is running close to the optical mode (8) and then is getting semilocalized again [curve (7)]. The definition of the semilocalized mode (6) is studied in Fig. 8(c). The junction $J(\varphi_x \simeq 105°)$ of this mode (6) with the localized mode (5) is of the same type as in Fig. 6(c). The junction S ($\varphi_x \simeq 112°$) of the mode with the localized mode (11) is displaying a much bigger increase in the density of states.

In the region between $\omega_{3A}(0)$ and $\omega_{1B}(\pi)$ we have also a resonance (9) and an antiresonance (10) similar to those obtained in Fig. 4 and discussed in Sec. IV A.

V. LOW-TEMPERATURE INTERFACE AND PLANAR DEFECT SPECIFIC HEAT

The surface contribution to the specific heat of a finite crystal has been studied extensively, both theoretically and experimentally.[1]

Some of the calculations of the low-temperature surface specific heat of a crystal were carried out for finite or semi-infinite isotropic elastic continua, giving qualitative[22,23] and quantitative[24-26] results. Other calculations[14,27-33] of the surface specific heat of a crystal which are lattice dynamical in character have also been published. The theoretical results are in good agreement with the experimental values[34] of the low-temperature surface specific heat obtained for NaCl powder.

However, to our knowledge the interface specific heat was not studied, neither theoretically nor experimentally. Recently we obtained[11] the low-temperature specific heat of the interface between two different crystals. This result was obtained in elasticity theory by the method proposed by Maradudin and Wallis.[29] Here we obtain it with

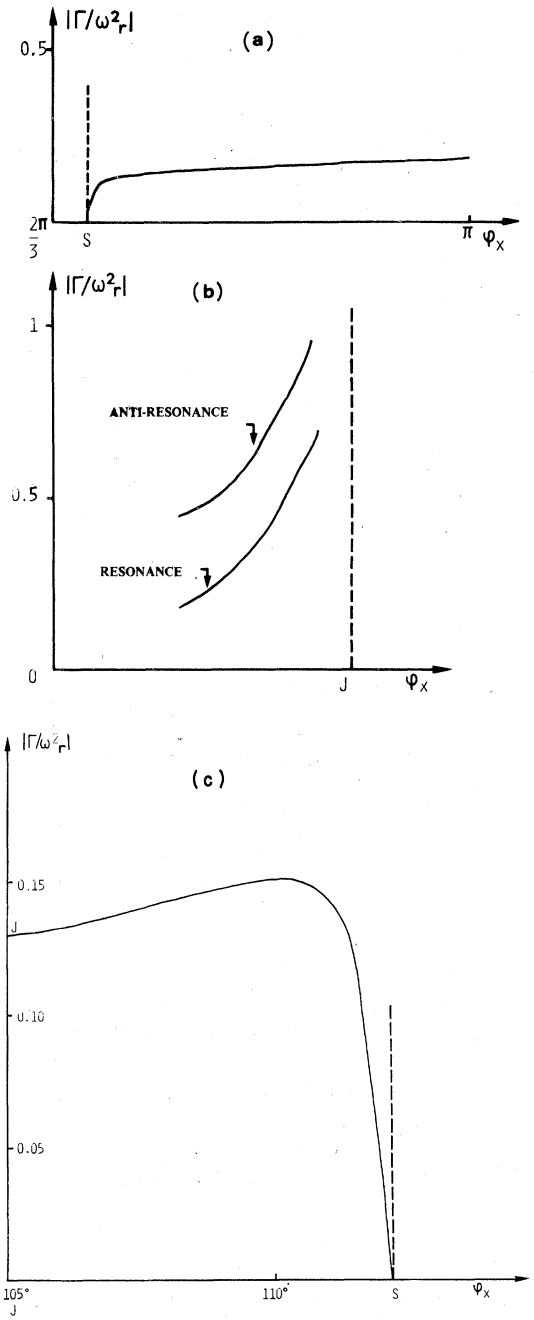

FIG. 8. Study as in Fig. 6 of the definition of some of the semilocalized and resonant modes given in Fig. 7. (a) Mode (1); (b) modes (2) and (3); (c) mode (6).

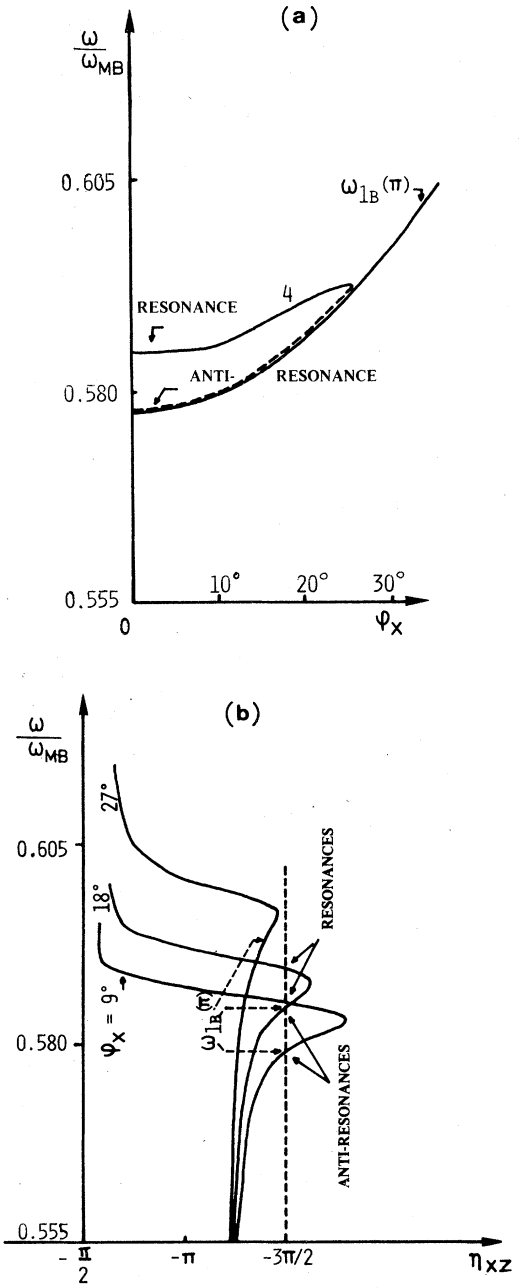

FIG. 9. Study of the definition of mode (4) given in Fig. 7. This mode is associated to an antiresonance—Fig. 9(a). In Fig. 9(b) we give the partial phase shift $\eta_{xz}(\varphi_x,\omega)$ near these modes for three values of φ_x.

the atomic model described above, which enables us to also derive the variation in the specific heat due to a planar defect.

Let us first describe the method used here (Sec. V A) before deriving the interface (Sec. V B) and the planar defect (Sec. V C) specific heats.

A. General formulation of the problem

Let us first recall the method introduced by Maradudin and Wallis[29] for the calculation of the surface specific heat at low temperatures.

In the harmonic approximation the specific heat of an arbitrary crystal can be written

$$C_v(T)=k_B\sum_i\frac{(\frac{1}{2}\beta\hbar\omega_i)^2}{(\sin h^2)(\frac{1}{2}\beta\hbar\omega_i)}$$

$$=k_B\sum_{n=1}^{\infty}n\sum_i(\beta\hbar\omega_i)^2e^{-n\beta\hbar\omega_i}, \tag{5.1}$$

where $\beta=(k_BT)^{-1}$, with T the absolute temperature and k_B is Boltzmann's constant; ω_i is the frequency of the ith normal mode, and the sum on i runs over all normal modes of the crystal. The second form of the expression for the specific heat is particularly convenient for its evaluation in the low-temperature limit where β is large.

To evaluate the sum on i in Eq. (5.1) we introduce for the two coupled crystals the function $F_I(y)$ by

$$F_I(y)=-\sum_i\frac{1}{y^2+\omega_i^2}. \tag{5.2}$$

We can write[29] for the difference between the specific heats of the two crystals before and after adhesion

$$\Delta C_v^{(a)}(T)=C_v^{(S)}(T)-C_v^{(I)}(T)$$

$$=\frac{2k_B(\beta\hbar)^2}{\pi}\sum_{n=1}^{\infty}n\int_0^{\infty}y^3\Omega(y)\sin n\beta\hbar y\,dy, \tag{5.3}$$

where we have put

$$\Omega(y)=F_S(y)-F_I(y), \tag{5.4}$$

$F_S(y)$ being the function given by Eq. (5.2) but for the two uncoupled crystals with their free surfaces.

Because n is greater than or equal to unity, and β is large, we require the asymptotic behavior of the integral

$$J=\int_0^{\infty}y^3\Omega(y)\sin n\beta\hbar y\,dy \tag{5.5}$$

in the limit as $n\beta\hbar\to+\infty$. Lighthill's theory of the asymptotic behavior of Fourier integrals[35] yields the result that if the function $\Omega(y)$ has as its only singularity a logarithmic dependence on $|y|$ in the limit as $y\to0$, i.e., if

$$\Omega(y)\sim-A\ln|y|+o(\ln|y|),\quad y\to0, \tag{5.6}$$

then the dominant term in the asymptotic expansion of the integral J in the limit $n\beta\hbar\to+\infty$ is

$$J \simeq -[3\pi A/(n\beta\hbar)^4] + o(n^{-4}), \quad n\beta\hbar \to +\infty. \tag{5.7}$$

It follows from Eqs. (5.3), (5.5), and (5.7) that the adhesion specific heat is given by

$$\Delta C_v^{(a)}(T) = -6A\zeta(3)k_B\left(\frac{k_BT}{\hbar}\right)^2 + o(T^2) \tag{5.8}$$

in the limit as $T \to 0$, where $\zeta(3)$ is the Riemann ζ function.

The problem of calculating the adhesion specific heat is therefore reduced to showing that the function $\Omega(y)$ associated with the adhesion between the two crystals has the asymptotic form given by Eq. (5.6) in the limit as $y \to 0$, and of determining the coefficient A.

From the definitions of $\Omega(y)$ and $F(y)$ [Eqs. (5.4) and (5.2)] it is easy to see that $\Omega(y)$ can be obtained from the knowledge of the Green's functions $\vec{\vec{G}}_I(\omega)$ and $\vec{\vec{G}}(\omega)$ for, respectively, two coupled and uncoupled crystals

$$\Omega(y) = \mathrm{Tr}[\vec{\vec{G}}_I(iy) - \vec{\vec{G}}(iy)]. \tag{5.9}$$

It is enough then to calculate the Green's functions before and after the introduction of the perturbation. This was done first by Maradudin and Wallis[29] for an atomic model of a surface and then in elasticity theory for a surface[33] and an interface.[11] Here we prefer, however, to use a slightly different and simpler approach.

The Green's functions $\vec{\vec{G}}_I(\omega)$ and $\vec{\vec{G}}(\omega)$ are related by

$$\vec{\vec{G}}_I = \vec{\vec{G}} + \vec{\vec{G}}\cdot\vec{\vec{V}}_I\cdot\vec{\vec{G}}_I, \tag{5.10}$$

where $\vec{\vec{V}}_I$ is the interface coupling. One can deduce from Eq. (5.10)

$$\det(\vec{\vec{I}} - \vec{\vec{V}}_I\cdot\vec{\vec{G}}) = \det(\vec{\vec{I}} - \vec{\vec{G}}_I\cdot\vec{\vec{V}}) = \frac{\det\vec{\vec{G}}}{\det\vec{\vec{G}}_I} = \frac{\prod_S(\omega^2 - \omega_S^2 + i\epsilon)^{-1}}{\prod_i(\omega^2 - \omega_i^2 + i\epsilon)^{-1}}. \tag{5.11}$$

And finally[36] with the definitions (5.2), (5.4), and (2.3):

$$\Omega(y) = -\left(\frac{1}{2\omega}\frac{d}{d\omega}\ln\Delta(\omega)\right)_{\omega=iy}. \tag{5.12}$$

It is simpler for an atomic model to obtain $\Omega(y)$ from Eq. (5.12) than from Eq. (5.9).

$\Delta(\omega)$ is obtained from $\Delta(\varphi_x, \varphi_y; \omega)$ by

$$\Delta(\omega) = \sum_{\varphi_x\varphi_y} \Delta(\varphi_x, \varphi_y; \omega). \tag{5.13}$$

B. Calculation of the interface specific heat

At low temperatures, the main contribution to the specific heat is due to the low-frequency modes. It is enough then to use the value of $\Delta(\varphi_x, \varphi_y; \omega)$ in the long-wavelength approximation. In Sec. III, we calculated $\Delta(\varphi_x, 0; \omega)$. But in the long-wavelength approximation, the Rosenzweig[2] model is isotropic. Therefore

$$\Delta(\varphi_x, 0; \omega) = \Delta(\varphi, \omega), \tag{5.14}$$

where

$$\varphi = (\varphi_x^2 + \varphi_y^2)^{1/2}. \tag{5.15}$$

We saw also [Eq. (2.4)] that Δ is the product of Δ_y and Δ_{xz}. The long-wavelength expansion of this last quantity was already given [Eqs. (3.8)–(3.10)]. The expression (3.3) of Δ_y takes the following form in the long-wavelength approximation:

$$\Delta_y(\varphi, \gamma) = [\alpha_A(1-\gamma)^{-1/2} + \alpha_B(1-\delta\gamma)^{-1/2}]\varphi^{-1} + o(\varphi^{-1}), \tag{5.16}$$

where we used the relation (3.7) between γ and ω^2 as well as the isotropy in the long-wavelength approximation ($\varphi_x \equiv \varphi$). Finally

$$\Delta(\varphi, \gamma) = \alpha_B^3\mathcal{E}(\gamma)[4\Delta_A(\gamma)\Delta_B(\gamma)\gamma^2]^{-1} \times [\alpha_A\alpha_B^{-1}(1-\gamma)^{-1/2} + (1-\gamma\delta)^{-1/2}]\varphi^{-3} + o(\varphi^{-3}) \tag{5.17}$$

where $\mathcal{E}(\gamma)$ is given by Eq. (3.9), $\Delta_A(\gamma)$ and $\Delta_B(\gamma)$ are given, respectively, by Eq. (3.11).

Owing to the isotropy in the elastic limit, $\Omega(y)$ [Eqs. (5.15) and (5.16)] can be calculated as

$$\Omega(y) = -\frac{S}{4\pi a^2}\left(\frac{1}{\omega}\frac{d}{d\omega}\int_0^{\varphi_c}\varphi\, d\varphi\, \ln\Delta(\varphi, \omega)\right)_{\omega=iy}, \tag{5.18}$$

where S is the interface area, S/a^2 is the number of atoms in a (001) plane, and φ_c is a cutoff. Such a cutoff arises naturally in a lattice theory, where the allowed values of φ are restricted to be inside the two-dimensional first Brillouin zone. We will find that $\Omega(y)$ has a logarithmic dependence on φ_c, in the limit as $|y| \to 0$, so that a precise value of φ_c is not needed for our purposes.

It is convenient to make the change of variable

$$\varphi = |y| ua/c_{tA}, \tag{5.19}$$

where $c_{tA} = a(2K_A/M_A)^{1/2}$ is the bulk transverse speed of sound in crystal A. Let us remark also that Eq. (3.2) can be rewritten

$$\delta = c_{tA}^2/c_{tB}^2 \tag{5.20}$$

with this change of variables, $\Omega(y)$ [Eq. (5.18)] becomes

$$\Omega(y) = \frac{S}{4\pi c_{tA}^2 y}\frac{d}{dy}\left(y^2\int_0^{c_{tA}k_c/|y|} du\, u F(u)\right), \tag{5.21}$$

where the expression for $F(u)$ can be deduced from Eqs. (5.17) and (5.18)

$$F(u)=\ln\left(\frac{\mathcal{E}(\gamma)}{\gamma^2\Delta_A(\gamma)\Delta_B(\gamma)}\right)+\ln[\alpha_A\alpha_B^{-1}(1-\gamma)^{-1/2}+(1-\gamma\delta)^{-1/2}]. \quad (5.22)$$

The quantity $F(u)$ is only function of u. Indeed when using the relation (3.7) between γ and ω^2, as well as $\omega=iy$ and the Eq. (5.19), one obtains

$$\gamma=-u^{-2}. \quad (5.23)$$

If it were necessary to evaluate the integral (5.21) exactly, the determination of $\Omega(y)$ would be a difficult problem indeed. Fortunately this is not the case. We require only the dominant term in $\Omega(y)$ in the limit as $|y|\to 0$. From Eq. (5.21) we see that $|y|$ appears only in the upper limit of the integral. This means that the small-$|y|$ behavior of $\Omega(y)$ is determined by the behavior of $uF(u)$ for large u. This is most easily seen by breaking up the range of integration $(0, c_{tA}k_c/|y|)$ into two intervals $(0,T)$ and $(T, c_{tA}k_c/|y|)$, where T is independent of y and large enough that an expansion of $F(u)$ in powers of u^{-2} is valid. Thus T should be greater than unity. The only y-dependent contribution to $\Omega(y)$ comes from the upper limit of the integral over the interval $(T, c_{tA}k_c/|y|)$, and the dominant contribution as $|y|\to 0$ arises from the leading term in the expansion of $F(u)$ in powers of u^{-2} for large u. After some algebra one obtains

$$uF(u)=C_1u-C_2u^{-1}+o(u^{-1}),$$

where C_1 and C_2 are independent of u and

$$C_2=\frac{2(K_B/K_A)^2+\frac{13}{4}(1+\delta)K_B/K_A+2\delta}{2(K_B/K_A)^2+5K_B/K_A+2}+\frac{1}{2}\frac{K_B/K_A+\delta}{K_B/K_A+1}. \quad (5.24)$$

Note that the first term in C_2 is contributed by the (x,z) modes and the second by the y modes.

We do not give C_1 explicitly, as only the term of order u^{-2} in $F(u)$ gives after integration a singular contribution to $\Omega(y)$ in the limit $y\to 0$. More precisely we obtain

$$\Omega(y)=\frac{SM_A}{4\pi a^2K_A}C_2\ln|y|+o(\ln|y|). \quad (5.25)$$

Finally with the help of Eqs. (5.6), (5.8), (5.24), and (5.25), we obtain the adhesion specific heat

$$\Delta C_v^{(a)}(T)=12\pi\frac{k_B^3}{\hbar^2}\frac{\zeta(3)}{C_{tA}^2}C_2ST^2+o(T^2). \quad (5.26)$$

The adhesion specific heat was defined as the difference between the specific heat of the two semi-infinite crystals and those of the bicrystal. We can also define an interface specific heat $\Delta C_v^{(i)}$ as the difference between the specific heat of the bicrystal and those of the same two crystals but infinite (without surfaces). These two entities are obviously related by

$$\Delta C_v^{(i)}=\Delta C_v^{(S)A}+\Delta C_v^{(S)B}-\Delta C_v^{(a)}, \quad (5.27)$$

where $\Delta C_v^{(S)l}$ $(l=A,B)$ is the surface specific heat of the crystal whose value[29] is for $C_l^2=3C_t^2$

$$\Delta C_v^{(S)l}=10\pi\frac{k_B^3}{\hbar^2}\frac{\zeta(3)}{C_{tl}^2}ST^2+o(T^2). \quad (5.28)$$

The result obtained here in the frame of an atomic model for the interface specific heat agrees with those obtained without the restrictive condition ($C_l^2=3C_t^2$) in elasticity theory.[11]

Let us note also that if we go to the limit of two identical crystals ($A\equiv B$), the above result boils down to

$$\Delta C_v^{(i)}=o(T^2). \quad (5.29)$$

In Sec. V C we will derive the variation of the specific heat due to a planar defect and show that it behaves like T^3 at low temperatures.

C. Specific heat of a planar defect

We derive here the specific heat $\Delta C_v(T)$ of a planar defect as the difference between the specific heat of a crystal with a planar defect and those of the same bulk crystal. The model is given by Fig. 1, but with $A\equiv B$. $\Delta C_v(T)$ can be obtained also here from Eqs. (5.3) and (5.12), where one substitutes $\Delta C_v(T)$ to $\Delta C_v^{(a)}(T)$, $\tilde{\Omega}(y)$ to $\Omega(y)$, and $\tilde{\Delta}(\omega)$ to $\Delta(\omega)$, with

$$\tilde{\Delta}(\omega)=\det[\vec{\vec{I}}-\vec{\vec{V}}_D\cdot\vec{\vec{G}}_0(\omega)], \quad (5.30)$$

where $\vec{\vec{V}}_D$ is the perturbation which creates a planar defect in an infinite crystal for which the Green's function is $\vec{\vec{G}}_0(\omega)$.

However, we will see that $\tilde{\Omega}(y)$ will not have here a logarithmic singularity like $\Omega(y)$ in (5.6). We will have therefore to use a different method than above for the calculation of $\Delta C_v(T)$. We adapt to this problem a method used by Maradudin *et al.*[36] for the calculation of the free energy of a defect at low temperatures. When integrating by parts several times Eq. (5.3) one obtains

$$\Delta C_v(T)=\frac{\pi}{3}k_B\frac{k_BT}{\hbar}\left[\Omega_1(0)-\tfrac{2}{5}\pi^2\Omega_1''(0)\left(\frac{k_BT}{\hbar}\right)^2+\frac{2\pi^4}{21}\Omega_1^{(4)}(0)\left(\frac{k_BT}{\hbar}\right)^4+\cdots\right], \quad (5.31)$$

where

$$\Omega_1(y)=\frac{d}{dy}\ln\tilde{\Delta}(\omega)\Big|_{\omega=iy} \quad (5.32)$$

and

$$\Omega_1^{(i)}(y) = \frac{d^i}{dy^i}\Omega_1(y). \tag{5.33}$$

In the same manner as we obtained Eq. (5.18) we obtain here

$$\Omega_1(y) = \frac{S}{2\pi a^2}\frac{d}{dy}\left(\int_0^{\varphi_c}\varphi\, d\varphi \ln\tilde{\Delta}(\varphi,\dot{\omega})\right)_{\omega=iy}. \tag{5.34}$$

As for the interface, we calculate $\tilde{\Delta}(\varphi_x,\varphi_y;\omega)$ for $\varphi_y=0$ and then use the isotropy of the Rosenzweig model in the long-wavelength limit to obtain $\tilde{\Delta}(\varphi;\omega)$, where $\varphi=(\varphi_x^2+\varphi_y^2)^{1/2}$. For $\varphi_y=0$, one has also here

$$\tilde{\Delta}(\varphi_x,\omega)=\tilde{\Delta}_y(\varphi_x,\omega)\Delta_{xz}(\varphi_x,\omega). \tag{5.35}$$

The expression of $\tilde{\Delta}_{xz}$ was given before[4] and was factorized in two parts corresponding, respectively, to symmetrical and antisymmetrical displacements, as the planar defect has a mirror plane of symmetry

$$\Delta_{xz}(\varphi,\omega)=\Delta_S(\varphi,\omega)\Delta_{AS}(\varphi,\omega) \tag{5.36}$$

with

$$\Delta_S(\varphi,\omega)=\alpha+\varphi\frac{1-\alpha}{\gamma}\left\{(1-\gamma)^{1/2}-\frac{3}{2}(3-\gamma)^{3/2}-\frac{1}{2}\left(\frac{3}{3-\gamma}\right)^{1/2}+\left(\frac{3-\gamma}{3}\right)^{1/2}+\frac{(1-\alpha)}{3}\left[\left(\frac{3}{3-\gamma}\right)^{1/2}-(1-\gamma)^{1/2}\right]\right\}+o(\varphi), \tag{5.37}$$

$$\Delta_{AS}(\varphi,\omega)=\alpha+\varphi\frac{1-\alpha}{6\gamma}\left(4[3(3-\gamma)]^{1/2}-\frac{3}{(1-\gamma)^{1/2}}-6(1-\gamma)^{1/2}-3(1-\gamma)^{3/2}\right)+o(\varphi), \tag{5.38}$$

where

$$\alpha=K'/K. \tag{5.39}$$

$\Delta_y(\varphi,\omega)$ can be easily obtained by transposition from a similar calculation done for the interface magnons.[15] The mathematics of this problem being identical to those of the y modes in the Rosenzweig model:

$$\tilde{\Delta}_y(\varphi,\omega)=\frac{1-(1-2\alpha)t}{t+1}\simeq\alpha+\varphi\frac{1-\alpha}{2}(1-\gamma)^{1/2}+o(\varphi), \tag{5.40}$$

where t is defined by Eq. (3.4).

Finally with the help of Eqs. (5.35)–(5.40), one obtains

$$\ln\tilde{\Delta}(\varphi,\omega)=3\ln\alpha+\varphi\frac{1-\alpha}{\alpha}\mathfrak{A}, \tag{5.41a}$$

where

$$\mathfrak{A}=\frac{1}{\gamma}\left\{(1-\gamma)^{1/2}-\tfrac{3}{2}(3-\gamma)^{3/2}-\frac{1}{2}\left(\frac{3}{3-\gamma}\right)^{1/2}+\left(\frac{3-\gamma}{3}\right)^{1/2}+\frac{1-\alpha}{3}\left[\left(\frac{3}{3-\gamma}\right)^{1/2}-(1-\gamma)^{1/2}\right]\right\}+\frac{1}{6\gamma}\left(4[3(3-\gamma)]^{1/2}-\frac{3}{(1-\gamma)^{1/2}}-6(1-\gamma)^{1/2}-3(1-\gamma)^{3/2}\right)+\tfrac{1}{2}(1-\gamma)^{1/2}. \tag{5.41b}$$

With the help of Eqs. (5.41) and (5.32), one can now calculate $\Omega_1(y)$. In this calculation, one has to substitute in to γ its value given by Eq. (3.7).

$$\gamma=\frac{M}{2K}\frac{\omega^2}{\varphi^2}=-\frac{M}{2K}\frac{y^2}{\varphi^2}. \tag{5.42}$$

Finally Eq. (5.31) enables us to see that the first nonvanishing term in the expression of $\Delta C_v(T)$ is of order T^3 and reads:

$$\Delta C_v(T)=\pi^2\frac{k_B^4}{\hbar^3}\frac{\mathfrak{B}(\alpha)}{C_t^3}aST^3+o(T^4), \tag{5.43a}$$

where

$$\mathfrak{B}(\alpha)=\frac{1-\alpha}{\alpha}\left\{\tfrac{4}{675}\left[\tfrac{29}{12}\sqrt{3}+\tfrac{99}{4}-\frac{1-\alpha}{3}\left(\frac{4}{\sqrt{3}}+9\right)\right]+\tfrac{1}{15}\right\}, \tag{5.43b}$$

where $C_t=(2K/M)^{1/2}a$ is the transverse speed of sound and a is the lattice parameter.

Note that the above expression is not valid for $\alpha=0$ (free surfaces), as then the expansions (5.37), (5.38), and (5.40) are no longer valid.

VI. CONCLUSIONS

In this paper, we recovered the Stoneley waves and their existence conditions. But we give also for the first time new types of vibrational interface modes.

In the elastic limit we found three different modes (see Figs. 4 and 7): the Stoneley wave or a new semilocalized mode (localized in one of the two crystals and resonant in the other); a new resonant mode (2), and a new antiresonant one (3). These modes may be excited by acoustical

methods used for Rayleigh waves.

In the optical region (top of the bulk bands and large wavelengths), we also indicate, for an interface between two monoatomic crystals, the possibility of existence of new modes. Some are of transverse character [see Figs. 2(a) and 2(b)], some correspond to motions inside the sagittal plane: mode (6) on Fig. (4) and mode (8) on Fig. 7. These modes could be excited by optical means.[21] Another important finding is the existence of interface gaps and windows for the same given value of $k_{\parallel}$ (see Figs. 4 and 7). Now interface modes may exist in these regions: modes (4), (5), and (7) on Fig. 4 and modes (5), (8), and (11) on Fig. 7. Such types of modes were discovered also in interface electronic excitations,[17,18,37] for metal-semiconductor junctions they are probably the states predicted by Bardeen.[38]

The considerations developed in Sec. IV about the relations between resonant, antiresonant, semilocalized, and localized states are probably rather general and characteristic of surface and interface problems. One can expect to find such effects in other than vibrational interface excitations. The fact that the resonant and semilocalized modes are, in general, well-defined features in the density of states, means that this mode may be observed directly and probably plays important roles in interface properties.

Finally the fact that we studied a coherent interface on an atomic level does not affect appreciably the result obtained for long wavelengths. The results obtained for short wavelengths will be of course influenced by interface roughness, dislocations, and diffusion. These interface defects will introduce couplings between the excitations of the bicrystal. The couplings can be expected to be roughly proportional to the concentration of interface defects and then treated as first-order corrections if the concentration of interface defects remain small.

We obtain also here for the first time on an atomic model the variation in the low-temperature specific heat due to a bicrystal interface and to a planar defect situated in the bulk of a crystal. The interface specific heat varies like T^2 at low temperatures and the specific heat due to a planar defect like T^3. From the experimental point of view, the measure of the interface specific heat should be possible as already mentioned in Sec. I. Our hope is that the theoretical results given here will stimulate some experimental work.

APPENDIX A: BULK GREEN'S FUNCTIONS

For the model defined in Sec. II, the bulk Green's function is

$$G_0(l_z,\sigma;l_z',\sigma')=\frac{1}{2\pi}\sum_j\int_{-\pi}^{+\pi}d\varphi_z\frac{e_\sigma(\varphi_x,j)\,e_{\sigma'}(\varphi_x,j)}{\omega^2-\omega_j^2(\varphi_z)+i\epsilon}, \tag{A1}$$

where the bulk eigenvalue $\omega_j^2(\varphi_z)$ and eigenvectors $e_\sigma(\varphi_x,j)$ are given by Eqs. (2.1) and (2.2).

In fact, we need here only the matrix elements of $\tilde{G}_0$ between l_z and $l_z'=0$ or 1. They were calculated[39] in a basis of symmetrical and antisymmetrical functions through the plane $l_z=\frac{1}{2}$, respectively

$$\left(\frac{|0x\rangle+|1x\rangle}{\sqrt{2}},\quad\frac{|0z\rangle-|1z\rangle}{\sqrt{2}},\quad\frac{|0y\rangle+|1y\rangle}{\sqrt{2}}\right)$$

and

$$\left(\frac{|0x\rangle-|1z\rangle}{\sqrt{2}},\quad\frac{|0z\rangle+|1z\rangle}{\sqrt{2}},\quad\frac{|0y\rangle-|1y\rangle}{\sqrt{2}}\right).$$

The matrix elements of $\tilde{G}_0$ between a symmetrical and antisymmetrical function are nil.

We will separate the real and imaginary part of $\tilde{G}_0$

$$G_{0\chi}(\sigma,\sigma')=R_\chi(\sigma,\sigma')+ig_\chi(\sigma,\sigma'), \tag{A2}$$

where χ stands for S (symmetrical) or AS (antisymmetrical).

Let us introduce the following notations:

$$\delta_i^{in}=\begin{cases}1, & \text{inside the band } i\\ 0, & \text{outside the band } i\end{cases}\qquad(i=1,2,3)$$

$$\delta_i^{out}=\begin{cases}-1, & \text{above the band } i\\ 0, & \text{inside the band } i\\ 1, & \text{below the band } i;\end{cases} \tag{A3}$$

$$V_i=|\omega^2-\omega_i^2(0)|^{1/2},$$

$$W_i=|\omega^2-\omega_i^2(\pi)|^{1/2},$$

$$B=4(K/M)(1+2\cos\varphi_x),\qquad(i=1,2,3)$$

$$C=8(K/M)(1+2\cos\varphi_x)[\omega^2\cos\varphi_x+4(K/M)\,(1-\cos\varphi_x)^2].$$

One has[39] the following results:

$$R_S^{xx}=\frac{2+\cos\varphi_x}{B}+\frac{1}{C}\left(\delta_1^{ex}(1+\cos\varphi_x)(1+2\cos\varphi_x)V_1W_1-\delta_3^{ex}(1-\cos\varphi_x)\frac{W_3^3}{V_3}\right),$$

$$J_S^{xx}=-\frac{1}{C}\left[\delta_1^{in}(1+\cos\varphi_x)(1+2\cos\varphi_x)V_1W_1+\delta_3^{in}(1-\cos\varphi_x)\frac{W_3^3}{V_3}\right],$$

$$G_{0S}^{xy}=G_{0S}^{yz}=G_{0S}^{yx}=G_{0S}^{zy}=0,\quad R_S^{yy}=\frac{1}{4K/M}\left(1-|\delta_2^{ex}|\frac{W_2}{V_2}\right),\quad J_S^{yy}=-\frac{\delta_2^{in}}{4K/M}\frac{W_2}{V_2},$$

$$R_S^{xz}=-\frac{\sin\varphi_x}{C}[\delta_1^{in}(1+2\cos\varphi_x)V_1W_1-\delta_3^{in}V_3W_3],\quad J_S^{xz}=-\frac{\sin\varphi_x}{B}-\frac{\sin\varphi_x}{C}[\delta_1^{ex}(1+2\cos\varphi_x)V_1W_1-\delta_3^{ex}V_3W_3],$$

$$R_S^{zz}=-\frac{\cos\varphi_x}{B}+\frac{1}{C}\left(\delta_1^{ex}(1-\cos\varphi_x)(1+2\cos\varphi_x)V_1W_1-\delta_3^{ex}(1+\cos\varphi_x)\frac{V_3^3}{W_3}\right)$$

$$J_S^{zz}=-\frac{1}{C}\left(\delta_1^{in}(1-\cos\varphi_x)(1+2\cos\varphi_x)V_1W_1+\delta_3^{in}(1+\cos\varphi_x)\frac{V_3^3}{W_3}\right),$$

$$R_{AS}^{xx}=-\frac{2+\cos\varphi_x}{B}+\frac{1}{C}\left(\delta_3^{ex}(1-\cos\varphi_x)V_3W_3-\delta_1^{ex}(1+\cos\varphi_x)(1+2\cos\varphi_x)\frac{V_1^3}{W_1}\right),$$

$$J_{AS}^{xx}=-\frac{1}{C}\left(\delta_1^{in}(1+\cos\varphi_x)(1+2\cos\varphi_x)\frac{V_1^3}{W_1}+\delta_3^{in}(1-\cos\varphi_x)V_3W_3\right),$$

$$G_{0AS}^{xy}=G_{0AS}^{yx}=G_{0AS}^{yz}=G_{0AS}^{zy}=0,\quad R_{AS}^{yy}=\frac{1}{4K/M}\left(-1+|\delta_2^{ex}|\frac{V_2}{W_2}\right),$$

$$J_{AS}^{yy}=\frac{-1}{4K/M}\delta_2^{in}\frac{V_2}{W_2},\quad R_{AS}^{zz}=\frac{\cos\varphi_x}{B}+\frac{1}{C}\left(\delta_3^{ex}(1+\cos\varphi_x)V_3W_3-\delta_1^{ex}(1-\cos\varphi_x)(1+2\cos\varphi_x)\frac{W_1^3}{V_1}\right),$$

$$J_{AS}^{zz}=-\frac{1}{C}\left(\delta_1^{in}(1-\cos\varphi_x)(1+2\cos\varphi_x)\frac{W_1^3}{V_1}+\delta_3^{in}(1+\cos\varphi_x)V_3W_3\right),\quad G_{0AS}^{xz}=-G_{0AS}^{zx}=-G_{0S}^{xz}.$$

APPENDIX B: SURFACE GREEN'S FUNCTIONS

Let us remove all bonds coupling the two semi-infinite crystals situated at $l_z\geq 1$ and $l_z\leq 0$. This creates a perturbation V_S in the dynamical matrix (see Sec. II). Taking due account of the translational symmetry parallel to the (001) surfaces, one obtains[2] for $\vec{\vec{V}}_S$ along the Δ axis ($\varphi_y=0$):

$$\vec{\vec{V}}_S=-2\frac{K}{M}\begin{array}{c}\begin{matrix}|0x\rangle & |0z\rangle & |1x\rangle & |1z\rangle & |0y\rangle & |1y\rangle\end{matrix}\\ \begin{bmatrix} 1 & 0 & -\cos\varphi_x & -i\sin\varphi_x & 0 & 0\\ 0 & 3 & -i\sin\varphi_x & -2-\cos\varphi_x & 0 & 0\\ -\cos\varphi_x & i\sin\varphi_x & 1 & 0 & 0 & 0\\ i\sin\varphi_x & -2-\cos\varphi_x & 0 & 3 & 0 & 0\\ 0 & 0 & 0 & 0 & 1 & -1\\ 0 & 0 & 0 & 0 & -1 & 1\end{bmatrix}\end{array}. \tag{B1}$$

The surface Green's function $\vec{\vec{G}}_S$ can be obtained from:

$$\vec{\vec{G}}_S=\vec{\vec{G}}_0+\vec{\vec{G}}_0\cdot\vec{\vec{V}}_S\cdot\vec{\vec{G}}_S. \tag{B2}$$

As there is no more interactions between the two semi-infinite crystals, the Green's function elements will be nonzero only for both l_z and l_z' ≥ 1 or ≤ 0.

In this paper, we need only $G_S(1,\sigma;1,\sigma')$ and $G_S(0,\sigma;0,\sigma')$.

Using Eq. (B2) we have:

$$G_S(1,\sigma;1,\sigma')=G_0(1,\sigma;1,\sigma')+\sum_{\sigma''=x,y,z}B_{\sigma''\sigma}G(1,\sigma'';1,\sigma'), \tag{B3a}$$

where

$$B_{x\sigma}=-(2K/M)[-\cos\varphi_x G_0(1,\sigma;0,x)-i\sin\varphi_x\, G_0(1,\sigma;0,z)+G_0(1,\sigma;1,x)],$$

$$B_{y\sigma}=-(2K/M)[-G_0(1,\sigma;0,y)+G_0(1,\sigma;1,y)],$$

$$B_{z\sigma} = -(2K/M)[-i\sin\varphi_x G_0(1,\sigma;0,x) - (2+\cos\varphi_x)\,G_0(1,\sigma;0,z) + 3G_0(1,\sigma;1,z)].$$

With the help of the elements of $\vec{\vec{G}}_0$ and noticing that

$$B_{xy} = B_{yx} = B_{zy} = B_{yz} = 0,$$

we can rewrite Eq. (B3) as:

$$G_S(1,y;1,\sigma') = [\delta\sigma', y/(1-B_{yy})]G_0(1,y;1,y), \tag{B4a}$$

$$G_S(1,x;1,x) = [(1-B_{zz})/\Delta]G_0(1,x;1,x), \tag{B5a}$$

$$G_S(1,z;1,z) = [(1-B_{xx})/\Delta]G_0(1,z;1,z), \tag{B6a}$$

$$G_S(1,x;1,z) = (B_{zx}/\Delta)G_0(1,z;1,z), \tag{B7a}$$

$$G_S(1,z;1,x) = (B_{xz}/\Delta)G_0(1,x;1,x), \tag{B8a}$$

where

$$\Delta = (1-B_{xx})(1-B_{zz}) - B_{xz}B_{zx}. \tag{B9a}$$

In the same manner, Eq. (B2) gives:

$$G_S(0,\sigma;0,\sigma') = G_0(0,\sigma;0,\sigma') + \sum_{\sigma''=x,y,z} \tilde{B}_{\sigma''\sigma} G(0,\sigma'';0,\sigma'), \tag{B3b}$$

where

$$\tilde{B}_{x\sigma} = -\frac{2K}{M}[G_0(0,\sigma;0,x) - \cos\varphi_x G_0(0,\sigma;1,x) + i\sin\varphi_x G_0(0,\sigma;1,z)],$$

$$\tilde{B}_{y\sigma} = -\frac{2K}{M}[G_0(0,\sigma;0,y) - G_0(0,\sigma;1,y)],$$

$$\tilde{B}_{z\sigma} = -\frac{2K}{M}[3G_0(0,\sigma;0,z) + i\sin\varphi_x G_0(0,\sigma;1,x) - (2+\cos\varphi_x)G_0(0,\sigma;1,z)].$$

And finally

$$G_S(0,y;0,\sigma') = [\delta\sigma', y/(1-\tilde{B}_{yy})]G_0(0,y;0,\sigma'), \tag{B4b}$$

$$G_S(0,x;0,x) = (1-\tilde{B}_{zz})G_0(0,x;0,x)/\tilde{\Delta}, \tag{B5b}$$

$$G_S(0,z;0,z) = (1-\tilde{B}_{xx})G_0(0,z;0,z)/\tilde{\Delta}, \tag{B6b}$$

$$G_S(0,x;0,z) = \tilde{B}_{zx}G_0(0,z;0,z)/\tilde{\Delta}, \tag{B7b}$$

$$G_S(0,z;0,x) = \tilde{B}_{xz}G_0(0,x;0,x)/\tilde{\Delta}, \tag{B8b}$$

where

$$\tilde{\Delta} = (1-\tilde{B}_{xx})(1-\tilde{B}_{zz}) - \tilde{B}_{xz}\tilde{B}_{zx}. \tag{B9b}$$

APPENDIX C: EXPRESSIONS OF $(\overleftrightarrow{I} - \overleftrightarrow{V}_I \cdot \overleftrightarrow{G})$

Let us first give the interface coupling matrix $\vec{\vec{V}}_I$, which is easily found by analogy with $\vec{\vec{V}}_S$ (Appendix B).

$$\vec{\vec{V}}_I = \frac{2K'}{M_B}\begin{array}{c} \\ |0x\rangle \\ |0z\rangle \\ |1x\rangle \\ |1z\rangle \\ |0y\rangle \\ |1y\rangle \end{array}\begin{array}{c} \begin{array}{cccccc} |0x\rangle & |0z\rangle & |1x\rangle & |1z\rangle & |0y\rangle & |1y\rangle \end{array} \\ \begin{pmatrix} 1 & 0 & -Q\cos\varphi_x & -iQ\sin\varphi_x & 0 & 0 \\ 0 & 3 & -iQ\sin\varphi_x & -Q(2+\cos\varphi_x) & 0 & 0 \\ -Q\cos\varphi_x & iQ\sin\varphi_x & Q^2 & 0 & 0 & 0 \\ iQ\sin\varphi_x & -Q(2+\cos\varphi_x) & 0 & 3Q^2 & 0 & 0 \\ 0 & 0 & 0 & 0 & 1 & -Q \\ 0 & 0 & 0 & 0 & -Q & Q^2 \end{pmatrix} \end{array}, \tag{C1}$$

where

$$Q = (M_B/M_A)^{1/2}. \tag{C2}$$

We also need the Green's function $\vec{\vec{G}}$ of the two semi-infinite crystals without interactions

$$G(l_z,\sigma;l_z',\sigma') = \begin{cases} G_S^A(l_z,\sigma;l_z',\sigma') & \text{if } l_z,\ l_z' \geq 1, \\ G_S^B(l_z,\sigma;l_z',\sigma') & \text{if } l_z,\ l_z' \leq 0, \\ 0 & \text{otherwise}. \end{cases} \tag{C3}$$

As the coupling $\vec{\vec{V}}_I$ acts only between the planes $l_z = 0$ and $l_z = 1$, we need here for the calculation of $(\vec{\vec{I}} - \vec{\vec{V}}_I \circ \vec{\vec{G}})$ only $G_S^A(1,\sigma;1,\sigma')$ and $G_S^B(0,\sigma;0,\sigma')$ which we gave in Appendix B. Finally

$$\vec{\vec{I}} - \vec{\vec{V}}_I \cdot \vec{\vec{G}} = \begin{pmatrix} (\vec{\vec{I}} - \vec{\vec{V}}_I \cdot \vec{\vec{G}})_{xz} & 0 \\ 0 & (\vec{\vec{I}} - \vec{\vec{V}}_I \cdot \vec{\vec{G}})_y \end{pmatrix}, \tag{C4}$$

where

$$(\vec{\vec{I}}-\vec{\vec{V}}_I\cdot\vec{\vec{G}})_{xz}=\vec{\vec{I}}-\frac{2K'}{M_B}\begin{bmatrix} |0x\rangle & |0z\rangle & |1x\rangle & |1z\rangle \\ G_S^B(0,x;0,x) & G_S^B(0,x;0,z) & -Q\cos\varphi_x G_S^A(1,x;1,x) & -Q\cos\varphi_x G_S^A(1,x;1,z) \\ & & -iQ\sin\varphi_x G_S^A(1,z,1,x) & -iQ\sin\varphi_x G_S^A(1,z;1,z) \\ 3G_S^B(0,z;0,x) & 3G_S^B(0,z;0,z) & -iQ\sin\varphi_x G_S^A(1,x;1,x) & -iQ\sin\varphi_x G_S^A(1,x;1,z) \\ & & -Q(2+\cos\varphi_x)G_S^A(1,z;1,x) & -Q(2+\cos\varphi_x)G_S^A(1,z;1,z) \\ -Q\cos\varphi_x G_S^B(0,x;0,x) & -Q\cos\varphi_x G_S^B(0,x;0,z) & Q^2G_S^A(1,x;1,x) & Q^2G_S^A(1,x;1,z) \\ +iQ\sin\varphi_x G_S^B(0,z;0,x) & +iQ\sin\varphi_x G_S^B(0,z;0,z) & & \\ iQ\sin\varphi_x G_S^B(0,x;0,x) & iQ\sin\varphi_x G_S^B(0,x;0,z) & 3Q^2G_S^A(1,z;1,x) & 3Q^2G_S^A(1,z;1,z) \\ -Q(2+\cos\varphi_x)G_S^B(0,z;0,x) & -Q(2+\cos\varphi_x)G_S^B(0,z;0,z) & & \end{bmatrix} \tag{C5}$$

and

$$(\vec{\vec{I}}-\vec{\vec{V}}_I\cdot\vec{\vec{G}})_y=\vec{\vec{I}}-\frac{2K'}{M_B}\begin{bmatrix} |0y\rangle & |1y\rangle \\ G_S^B(0,y;0,y) & -QG_S^A(1,y;1,y) \\ -QG_S^B(0,y;0,y) & Q^2G_S^A(1,y;1,y) \end{bmatrix}. \tag{C6}$$

APPENDIX D: EXPRESSIONS OF $\Delta_y(\varphi_x,\omega)$, $\Delta_{xz}(\pi,\omega)$, AND $\Delta_{xz}(0,\omega)$

1. $\Delta_y(\varphi_x,\omega)$

With the help of Eqs. (2.1), (2.2), and (A1), one easily obtains:

$$G_0(l_z,y;l'_z,y)=\frac{M}{2K}\,\frac{t_y^{1+|l_z-l'_z|}}{t_y^2-1}, \tag{D1}$$

where

$$t_\sigma=\begin{cases}\zeta_\sigma-(\zeta_\sigma^2-1)^{1/2} & \text{if } \zeta_\sigma>1,\\ \zeta_\sigma+i(1-\zeta_\sigma^2)^{1/2} & \text{if } -1<\zeta_\sigma<1,\\ \zeta_\sigma+(\zeta_\sigma^2-1)^{1/2} & \text{if } \zeta_\sigma<-1,\end{cases} \tag{D2}$$

with

$$\zeta_y=2-\cos\varphi_x-M\omega^2/4K. \tag{D3}$$

The corresponding surface Green's function can then be obtained from Eqs. (B4):

$$G_S(1,y;1,y)=G_S(0,y;0,y)=(M/2K)[t_y/(t_y-1)]. \tag{D4}$$

We can now calculate $\Delta_y(\varphi_x,\omega)$ with the help of Eq. (C6)

$$\Delta_y(\varphi_x,\omega)=1-\alpha_A t_{yA}/(t_{yA}-1)-\alpha_B t_{yB}/(t_{yB}-1), \tag{D5}$$

where α_A and α_B are defined by Eq. (3.1).

2. $\Delta_{xz}(\pi,\omega)$

For $\varphi_x=\pi$ and $\varphi_y=0$, modes 1 and 3 are also decoupled and one has from Eqs. (B7) and (B8):

$$G_S^A(1,x;1,z)=G_S^A(1,z;1,x)=G_S^B(0,x;0,z)=G_S^B(0,z;0,x)=0 \tag{D6}$$

and also

$$\Delta_{xz}(\pi,\omega)=\Delta_x(\pi,\omega)\,\Delta_z(\pi,\omega). \tag{D7}$$

As above, one obtains

$$G_0(l_z,x;l'_z,x)=-(M/2K)[t_x^{1+|l_z-l'_z|}/(t_x^2-1)], \tag{D8}$$

where t_x is given by Eq. (D2) with

$$\zeta_x=M\omega^2/4K-5. \tag{D9}$$

Similarly

$$G_0(l_z,z;l'_z,z)=(M/2K)[t_z^{1+|l_z-l'_z|}/(t_z^2-1)], \tag{D10}$$

where t_z is also given by Eq. (D2) with

$$\zeta_z=3-M\omega^2/4K. \tag{D11}$$

Finally with the help of Eq. (C5)

$$\Delta_x(\pi,\omega)=1-\alpha_B t_{xB}/(t_{xB}+1)-\alpha_A t_{xA}/(t_{xA}+1), \tag{D12}$$

$$\Delta_z(\pi,\omega)=1-3\alpha_A\frac{t_{zA}}{3t_{zA}-1}-3\alpha_B\frac{t_{zB}}{3t_{zB}-1}+8\alpha_A\alpha_B\frac{t_{zA}t_{zB}}{(3t_{zA}-1)(3t_{zB}-1)}. \tag{D13}$$

3. $\Delta_{xz}(0,\omega)$

Here also, we have the decoupling between modes x and z, and as a consequence the relations (D6), as well as

$$\Delta_{xz}(0,\omega)=\Delta_x(0,\omega)\,\Delta_z(0,\omega). \tag{D14}$$

In the same manner as above, one obtains:

$$G_0(l_z,x;l'_z,x)=(M/2K)[\tilde{t}_x^{1+|l_z-l'_z|}/(\tilde{t}_x^2-1)], \tag{D15}$$

$$G_0(l_z,z;l'_z,z)=(M/6K)[\tilde{t}_z^{1+|l_z-l'_z|}/(\tilde{t}_z^2-1)], \tag{D16}$$

where $\tilde{t}_x$ and $\tilde{t}_z$ are defined by Eqs. (D2) but now with

$$\tilde{\zeta}_x=1-M\omega^2/4K, \tag{D17}$$

$$\tilde{\zeta}_z=1-M\omega^2/12K. \tag{D18}$$

Finally with the help of Eq. (C5)

$$\Delta_x(0,\omega)=1-\alpha_A\tilde{t}_{xA}/(\tilde{t}_{xA}-1)-\alpha_B\tilde{t}_{xB}/(\tilde{t}_{xB}-1), \tag{D19}$$

$$\Delta_z(0,\omega)=1-\alpha_A\tilde{t}_{zA}/(\tilde{t}_{zA}-1)-\alpha_B\tilde{t}_{zB}/(\tilde{t}_{zB}-1). \tag{D20}$$

---

*Present address: Centre d'Etudes d'Electronique des Solides, associé au CNRS, Université de Science et Techniques du Languedoc, Place Eugène Battaillon 34060 Montpellier Cédex, France.

† Equipe de recherche associée au Centre National de la Recherche Scientifique.

[1]See for example R. F. Wallis, Prog. Surf. Sci. 4, 233 (1974).

[2]L. N. Rosenzweig, Uchenge Zap. Hark Gos. Univ. Tr. Fiz. Mat. Otdel 2, 19 (1950).

[3]P. Masri and L. Dobrzynski, Surf. Sci. 34, 119 (1973).

[4]P. Masri and L. Dobrzynski, J. Phys. (Paris) 36, 551 (1975).

[5]M. Lifshitz and A. M. Kosevich, Rep. Prog. Phys. 29, 217 (1966).

[6]Ya. A. Iosilevskiy, Kristallografiya, 14, 201 (1969).

[7]Ya. A. Isoilevskiy and R. A. Vardanyan, Fiz. Met. Metalloved. 33, 1164 (1972).

[8]E. W. Montroll and R. B. Potts, Phys. Rev. 100, 525 (1955).
[9]W. Ludwig, Springer Tracts Mod. Phys. 43, 206 (1967); W. Ludwig and B. Lengeler, Solid State Commun. 2, 83 (1964).
[10]R. Stoneley, Proc. R. Soc. A 106, 421 (1927).
[11]B. Djafari-Rouhani and L. Dobrzynski, Phys. Rev. B 14, 2296 (1976).
[12]See, for example, P. Lenglart, L. Dobrzynski, and G. Leman, Ann. Phys. (Paris) 7, 407 (1972).
[13]P. Masri and L. Dobrzynski, J. Phys. (Paris) 32, 295 (1971) and J. Phys. Chem. Solids 34, 847 (1973).
[14]L. Dobrzynski and D. L. Mills, J. Phys. Chem. Solids, 30, 1043 (1969).
[15]B. Djafari-Rouhani and L. Dobrzynski, J. Phys. (Paris) 36, 835 (1975).
[16]G. Allan, M. Lannoo, and L. Dobrzynski, Philos. Mag. 30, 33 (1974).
[17]L. Dobrzynski, S. Cunningham, and H. Weinberg, Surf. Sci. (to be published).
[18]J. P. Muscat, G. Allan, and M. Lannoo (unpublished).
[19]J. G. Scholte, Proc. Acad. Sci. Amst. 45, 20 (1942), 45, 159 (1942).
[20]A. Defebvre and J. Pouliquen, Ultrasonics International Conference Proceedings, 1975, p. 129 (unpublished).
[21]F. Proix and R. Racek, *Proceedings du Colloque de Physique et de Chimie des Surfaces* (Le Vide, Paris, 1973), p. 70, Vols. 163–165.
[22]A. Kh. Breger and A. A. Zhukhovtskii, J. Phys. Chem. USSR 20, 1459 (1946); Acta Physicochim. USSR 21, 1001 (1946); J. Chem. Phys. 14, 569 (1946).
[23]E. W. Montroll, J. Chem. Phys. 18, 183 (1950).
[24]R. Stratton, Philos. Mag. 44, 519 (1953); J. Chem. Phys. 37, 2972 (1962).
[25]M. Dupuis, R. Mazo, and L. Onsager, J. Chem. Phys. 33, 1452 (1960).
[26]M. G. Burt, J. Phys. C 6, 855 (1973).
[27]D. Patterson, Can. J. Chem. 33, 1079 (1955).
[28]L. Dobrzynski and G. Leman, J. Phys. (Paris) 30, 116 (1969).
[29]A. A. Maradudin and R. F. Wallis, Phys. Rev. 148, 945 (1966).
[30]R. E. Allen and F. W. De Wette, J. Chem. Phys. 51, 4820 (1969).
[31]T. S. Chen, G. P. Alldredge, F. W. De Wette, and R. E. Allen, J. Chem. Phys. 55, 3121 (1971); G. P. Alldredge, T. S. Chen, and F. W. De Wette, *Proceedings of the Thirteenth International Conference on Low-Temperature Physics, Boulder, Colorado,* 1972, edited by R. H. Kropschot and K. D. Timmerhaus (Colorado U. P., Boulder, Colo., 1973).
[32]S. L. Cunningham, Sur. Sci., 33, 139 (1972).
[33]L. Dobrzynski and A. A. Maradudin, Phys. Rev. B 14, 2200 (1976).
[34]J. H. Barkman, R. L. Anderson, and T. E. Brackett, J. Chem. Phys. 54, 2605 (1971).
[35]M. J. Lightill, *Fourier Analysis and Generalized Functions* (Cambridge U. P., Cambridge, 1958), Chap. IV.
[36]See also: A. A. Maradudin, E. W. Montroll, G. H. Weiss, and I. P. Ipatova, Solid State Phys. Suppl. 3, 390 (1971).
[37]S. G. Lowe and M. L. Cohen, Phys. Rev. Lett. 35, 866 (1975).
[38]J. Bardeen, Phys. Rev. 71, 717 (1947).
[39]P. Masri, Thesis (Orsay, 1971) (unpublished).